

NASA CR-179459

ADVANCED OPTICAL SMOKE METERS FOR JET ENGINE EXHAUST MEASUREMENT

(NASA-CR-179459) ADVANCED OPTICAL SMOKE METERS FOR JET ENGINE EXHAUST MEASUREMENT
Final Report (General Electric Co.) 43 p
CSCL 14B
N87-12829
Unclas
G3/35 44651

Prepared by

Robert W. Pitz

**General Electric Company
Corporate Research and Development
Schenectady, New York 12301**

Prepared for

**National Aeronautics and Space Administration
Lewis Research Center
21000 Brookpark Road
Cleveland, Ohio 44135**

CONTRACT NAS3-24084



NASA CR-179459

**ADVANCED OPTICAL SMOKE METERS FOR
JET ENGINE EXHAUST MEASUREMENT**

Prepared by

Robert W. Pitz

**General Electric Company
Corporate Research and Development
Schenectady, New York 12301**

Prepared for

**National Aeronautics and Space Administration
Lewis Research Center
21000 Brookpark Road
Cleveland, Ohio 44135**

CONTRACT NAS3-24084

TABLE OF CONTENTS

Section		Page
	Nomenclature	iv
	Summary	1
1	Introduction	2
2	Experimental Evaluation of the Smoke Meter Concepts	4
	2.1 Modulated Transmission (MODTRAN)	4
	2.1.1 General Description	4
	2.1.2 Theoretical Principles	4
	2.1.3 Experimental Setup	8
	2.1.4 Nitrogen Dioxide Measurements	10
	2.1.5 Smoke Measurement	11
	2.1.6 Evaluation	15
	2.2 Photothermal Deflection Spectroscopy (PDS)	16
	2.2.1 General Description	16
	2.2.2 Theoretical Principles	16
	2.2.3 Experimental Setup	19
	2.2.4 Nitrogen Dioxide Measurements	19
	2.2.5 Smoke Measurement	21
	2.2.6 Evaluation	25
3	Summary and Conclusions	28
	Appendix	31
	References	32

PRECEDING PAGE BLANK NOT FILMED

NOMENCLATURE

a	Radius of the pump beam (m)
A_A	Specific absorption coefficient of smoke (m^2/g)
A_E	Specific extinction coefficient of smoke (m^2/g)
$A_{\text{H}_2\text{O}}$	Specific absorption coefficient of water (m^2/g)
A_{NO_2}	Specific extinction (or absorption) coefficient of NO_2 (m^2/g)
b_a	Optical absorption (m^{-1})
C	Optical constant
d	Particle diameter (μm)
f	Modulation frequency (Hz)
I	Transmitted light power (W)
I_N	Transmitted light power through optical elements (W)
I_o	Original light power of source (W)
k	Thermal conductivity (W/m-K)
l_d	Diffusion length (m)
L	Optical path length (m)
m	Complex index of refraction
n	Real part of the index of refraction
p	Gas pressure (Pa)
R	Radial distance to detector (m)
T	Temperature (K)
T_w	Average transmission of the optical elements
x_o	Beam separation distance (m)

Greek Letters

α	Thermal diffusivity
γ	Ratio of specific heats
λ	Wavelength (nm)
ρ	Soot concentration (mg/m^3)
ρ_c	Solid density of carbon in soot (g/cm^3)
ρ_g	Gas density (kg/m^3)
$\rho_{\text{H}_2\text{O}}$	Water concentration (g/m^3)
ρ_{NO_2}	NO_2 density (kg/m^3)

σ_a Absorption cross section (cm^2)
 ϕ Beam crossing angle (radians)

Subscripts

o Reference conditions
rms Root mean square value of a variable

Superscripts

' Fluctuating value of a variable

SUMMARY

Smoke meters with increased sensitivity, improved accuracy, and rapid response are needed to measure the smoke levels emitted by modern jet engines. The standard soiled tape meter in current use is based on filtering, which yields long-term averages and is insensitive to low smoke levels. Two new optical smoke meter techniques that promise to overcome these difficulties have been experimentally evaluated: modulated transmission (MODTRAN) and photothermal deflection spectroscopy (PDS). Both techniques are based on light absorption due to smoke, which is closely related to smoke density. They are variations on direct transmission measurements which produce a modulated signal that can be easily measured with phase sensitive detection. The MODTRAN and PDS techniques were tested on low levels of smoke and diluted samples of NO_2 in nitrogen, simulating light absorption due to smoke. The results are evaluated against a set of ideal smoke meter criteria that include a desired smoke measurement range of 0.1 to 12 mg/m^3 (smoke numbers of 1 to 50) and a frequency response of 1 per second. The MODTRAN instrument is found to be inaccurate for smoke levels below 3 mg/m^3 and is able to make a measurement only about once every 20 seconds because of its large sample cell. The PDS instrument meets nearly all the characteristics of an ideal smoke meter: it has excellent sensitivity over a range of smoke levels from 0.1 to 20 mg/m^3 (smoke numbers of 1 to 60) and good frequency response (1 per second).

Section 1

INTRODUCTION

As early as 1960, jet engine smoke emissions were a concern because of the detectability of black smoke trails from military aircraft. Later, smoke emissions from commercial jet aircraft traffic near metropolitan airports, particularly during landings and takeoffs, were the object of studies assessing aircraft contributions to air pollution.¹ These problems are an ongoing concern, and low smoke emissions are a primary goal of the jet engine designer. For military aircraft, the engine designer must meet the often conflicting goals of low smoke emissions and high altitude reflight capability. The use of broader specification aircraft fuels (which often increase smoke emissions) promises to exacerbate these problems with the added concern of higher radiative loading of the combustion liner.

Efforts to control and reduce smoke emissions through new engine design and control technology are a continuing pursuit. These investigations have focused on both combustor design² and fuel additives³ to reduce smoke emissions. Such efforts require accurate measurements to quantify smoke levels from jet engine exhausts. Smoke meters in current use are based on filtering techniques,^{4,5} which yield only long-term averages. These techniques require lengthy and costly engine tests, and the data reduction for them may take days to complete. Methods are needed to achieve increased range, improved accuracy, and faster response.

With the recent advances in optical and laser measurements, alternate methods are starting to emerge for measurement of smoke levels. For example, laser-induced photoacoustic spectroscopy has been used to make measurements of soot from diesel exhausts.^{6,7} Although diesel exhausts generally have higher smoke levels than those encountered in jet engines, optical techniques such as photoacoustic spectroscopy are promising candidates for accurate, rapid, and sensitive measurement of smoke from jet engines.

In view of these advances, a recent study⁸ was undertaken to analyze these new techniques and assess current technology for application to jet engine smoke measurement. A set of criteria were determined to characterize an ideal jet engine smoke meter called the "General Smoke Meter Requirements" (see Appendix A), and all the potential smoke measurement techniques were judged against these criteria. After an evaluation of a wide range of smoke meter concepts including commercial instruments, five smoke measurement techniques were considered in detail. Four optical techniques were studied: Modulated Transmission (MODTRAN), Cross Beam Absorption Counter (CBAC), Laser Induced Incandescence (LIN), and Photoacoustic Spectroscopy (PAS). A rapid response filter instrument called a Taper Element Oscillating Microbalance (TEOM) was also evaluated.

The description and analysis of the five most promising techniques are discussed in detail in Reference 8, and only a few details will be given here. The MODTRAN technique was judged the most promising candidate for jet engine smoke measurement. The MODTRAN technique is a variation on a direct transmission measurement in which smoke is passed through a transmission cell and the smoke density is modulated by a loudspeaker. The fluctuating component of the optical transmission is measured; this value is directly proportional to the light extinction and the smoke density. The primary advantage of the technique is that the signal is directly related to the smoke density and insensitive to window contamination. The other four techniques were ranked much lower than the MODTRAN instrument except for the TEOM instrument, which was judged to be a good secondary standard as it is commercially available.

The "General Smoke Meter Requirements" given in Appendix A have been found to be a good basis for evaluation. This set of requirements is identical to those used in the first study⁸ except for a modification of the smoke range of interest to 0.1–12 mg/m³ (smoke numbers, SN = 1-50). In the earlier study, the ideal smoke meter had a measurement range of 1-100 mg/m³ (SN = 10-85). Because of design improvements, jet engines of current interest have a lower range of smoke levels. This can be seen in Figure 1-1, where some measurements of jet engine smoke and the corresponding visibility characteristics are shown. Much of this data is for older engines, but the TF39-LS engine (a forerunner of modern bypass engines such as the CF6-80) has a low smoke level (1 mg/m³, SN = 10) characteristic of new jet engines.

Newer engines generally have smoke levels of 2 mg/m³ (SN=20) and below. Because of the lack of sensitivity of current standard soiled tape smoke meters,⁵ smoke levels below 1 mg/m³ (SN = 10) cannot be measured accurately. For example, Champagne⁹ has measured the uncertainty of the soiled tape meter at a low smoke level of 0.4 mg/m³ (SN = 5) to be SN = 5±4 (a smoke density variation of 0.1 to 1 mg/m³). The ideal smoke meter should have a lower limit sensitivity of 0.1 mg/m³ (SN = 1) because levels this low are thought to exist in the exhaust of new high-bypass jet engines. The upper level of the smoke measurement range is set by the needs of engine component development. Advanced experimental combustors may produce higher smoke levels but seldom above 12 mg/m³ (SN = 50). Thus a more appropriate smoke meter range of 0.1-12 mg/m³ is specified in the "General Smoke Meter Requirements" (Appendix A).

In this study two potential smoke meter techniques are experimentally evaluated: the most promising technique of the previous study, MODTRAN, and a new technique not previously considered, photothermal deflection spectroscopy (PDS). The performance of these smoke meters is compared against the "General Smoke Meter Requirements."

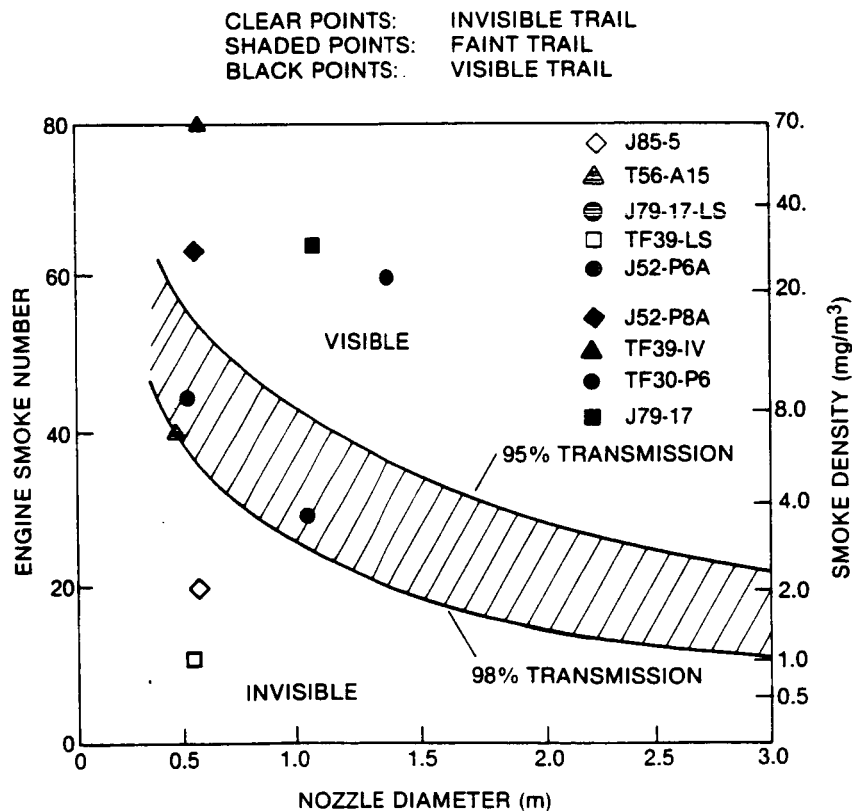


Figure 1-1. Jet engine smoke density and visibility correlation

Section 2

EXPERIMENTAL EVALUATION OF THE SMOKE METER CONCEPTS

In the following sections, two smoke meters whose signal is proportional to the visible light absorption of soot are experimentally evaluated: modulated transmission (MODTRAN) and photothermal deflection spectroscopy (PDS). Optical techniques generally have a fast response, which is a desirable quality in a new smoke meter. Smoke meters based on light absorption by smoke have the advantage that the signal is closely related to smoke density and insensitive to particle size. Optical scattering techniques do not offer this advantage. In the experimental evaluation both optical techniques are directly compared to the standard soiled tape meter and the tapered element oscillating microbalance (TEOM) while measuring smoke.

2.1 MODULATED TRANSMISSION (MODTRAN)

2.1.1 General Description

Direct transmission measurements of soot extinction have the advantages of simplicity and a close relationship to the desired measurement quantity—soot loading in units of mass per unit volume. However, soot levels of 1 mg/m^3 attenuate light at about 1% per meter, which is very difficult to measure with direct transmission because of window contamination and detector instabilities. Modulated transmission (MODTRAN) is a variation on direct transmission in which the sample gas is passed through a cell and the gas density is modulated acoustically by a loudspeaker. The only value measured is the fluctuating component of the light transmission, which is directly proportional to the light extinction and insensitive to window contamination. Accurate, sensitive measurements of light extinctions of 1% and below are possible.

A typical modulated transmission configuration is shown in Figure 2-1. A source such as an incandescent bulb, filtered to the desired color bandwidth, is focused through a gas cell where the soot sample is subjected to a moderately intense acoustic wave. The cell is closed at one end and driven at a resonant frequency in a high order mode by a loudspeaker at the other end. The light beam traverses a region of maximum gas density fluctuation, while the soot sample is admitted and exhausted by ports near regions of minimum fluctuation density, minimizing perturbation of sample lines by the acoustic field in the cell. The transmitted light beam is detected by a silicon photodiode. The small amplitude variation in the photodiode signal (typically 10^{-5} to 10^{-6} of the average level) resulting from the acoustic modulation of the soot absorber density can be determined quantitatively from the output of a lock-in amplifier that uses the loudspeaker drive or a pressure transducer signal as a reference signal. The analysis of this system, developed below, shows that soot mass concentration can be determined from the following quantities: the rms variation and the average value of the photodetector signal, a measure of the rms acoustic pressure fluctuation, and the specific extinction coefficient of soot. A combined calibration constant of the detectors can be determined by filling the cell with a known concentration of absorber gas (such as NO_2).

2.1.2 Theoretical Principles

The light power (W) transmitted through an absorbing medium in a cell such as shown in Figure 2-1 is given by Beer's law:*

* Also known as Bouguer's law or the Beer-Lambert equation.

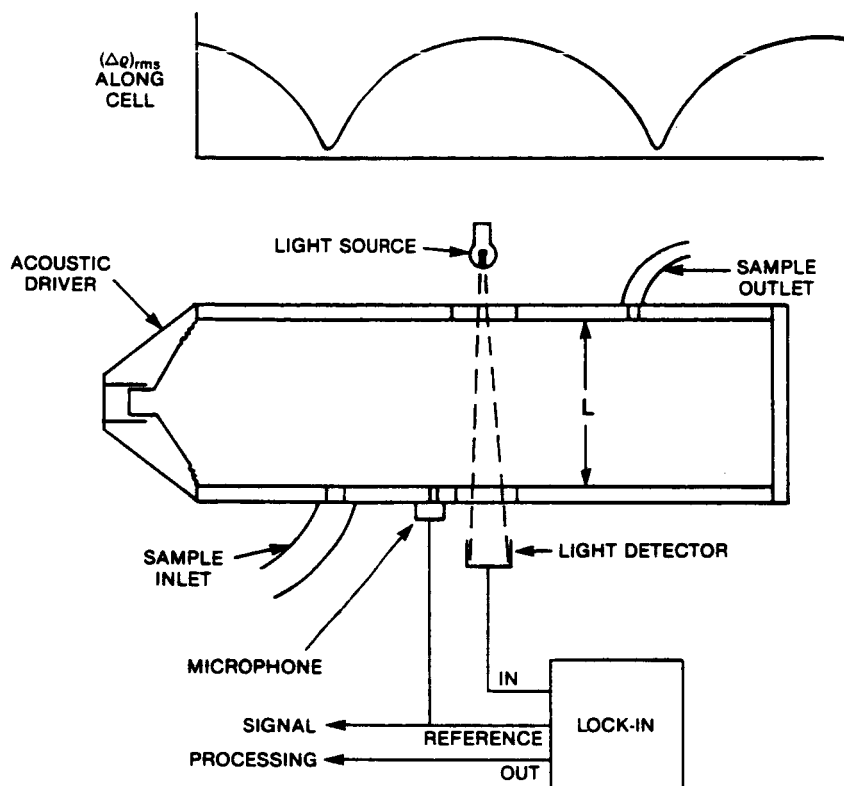


Figure 2-1. System configuration for modulated transmission measurement of soot concentration

$$I = I_o T_w \exp(-A_E \rho L) \quad (2-1)$$

I_o is the original light power, T_w is the transmission of the optical elements (i.e., windows), A_E is the specific extinction coefficient (sum of the absorption and scattering coefficients expressed in m^2/g), ρ is the mass concentration of the soot in the gas and L is the path length of the light through the cell.

In a practical sense, Beer's Law is valid for monochromatic radiation over negligible to moderate optical depth (typically, $0 \leq A_E \rho L \leq 3$). The upper limit on optical depth arises because of multiple scattering, which can return part of the light originally diverted from the beam by scattering. When broadband radiation is involved, Beer's Law must be integrated over wavelength, taking into account the variation of A_E with wavelength. However, in our case $A_E \rho L$ is expected to be small ($\ll 1$) at all probed wavelengths, so that the first two terms of the Taylor series expansion of $\exp(-A_E \rho L)$ are sufficient. In this case the value of A_E given by,

$$\bar{A}_E = \frac{\int I_o(\lambda) A_E(\lambda) d\lambda}{\int I_o(\lambda) d\lambda} \quad (2-2)$$

can be used with Beer's Law with negligible error. Here $A_E(\lambda)$ and $I_o(\lambda)$ are the values of the specific extinction and the source intensity as a function of wavelength.

In modulated transmission the density in the cell is modulated. The transmitted light power is given by,

$$I + I'(t) = I_0 [T_w + T_w'(t)] \exp [-(\rho + \rho'(t)) A_E L] \quad (2-3)$$

Here I is the value of the transmitted light averaged over a measurement period (typically one second for this application) while $I'(t)$ is the fluctuation. The factors T_w and $T_w'(t)$ account for the average and fluctuation of transmission through optical elements, and ρ and $\rho'(t)$ are the average and fluctuating values of the soot mass concentration. In this application the desired measured quantity is the averaged soot mass concentration, ρ , or the extinction per unit length, ρA_E . As noted above, we are primarily concerned with measurement of weak absorption values (e.g., 1% extinction or less, across a 10 cm path), and consequently, it is accurate to expand the fluctuation of the exponential function in Equation 2-3 into its first two terms, i.e.,

$$I + I'(t) = I_0 [T_w + T_w'(t)] [1 - \rho A_E L (1 + \rho'(t)/\rho)] \quad (2-4)$$

For adiabatic, isentropic, expansion/compression cycles, the gas density fluctuations are given by (assuming $\rho_g' \ll \rho_g$),

$$\rho_g'(t)/\rho_g = p'(t)/(\gamma p) \quad (2-5)$$

where $\rho_g'(t)$ and ρ_g are the average and fluctuating values of the gas density and p and $p'(t)$ are the average and fluctuating values of gas pressure, while γ is the ratio of specific heats ($\gamma = 1.4$ for N_2).

The smoke particle mass fraction will fluctuate similarly to the gas. Calculations of particle motion in turbulent gas flows (Melling and Whitelaw¹⁰) that have been checked experimentally (Mazumder and Kirsch¹¹) indicate that 1.3 μm diameter TiO_2 particles will follow the velocity fluctuations up to 1 kHz with 99% fidelity. Soot particles have a density of 1 g/cm^3 , which is less than half that of TiO_2 , and also have a greater frequency response. Thus soot particles in the size of interest (0.01 – 1.0 μm) will follow the gas pressure fluctuations up to 1 kHz. The soot density fluctuations, $\rho'(t)/\rho$, are given by the right-hand side of Equation 2-5. Substituting into Equation 2-4 we have,

$$I + I'(t) = I_0 [T_w + T_w'(t)] [1 - \rho A_E L (1 + p'(t)/(\gamma p))] \quad (2-6)$$

A likely measurement procedure based on Equation 2-6 would involve determination of the root-mean-square (rms) fluctuation of $I'(t)$ in a narrow frequency band around the acoustic frequency--a standard operation performed by a lock-in amplifier. Therefore we separate the signal into its mean and time varying components. The mean signal is given by

$$I = I_0 T_w (1 - A_E \rho L) \quad (2-7)$$

and represents the direct transmission measurement in the small extinction limit. The time varying signal is given by,

$$I'(t) = - I_0 [T_w \rho A_E L p'(t)/(\gamma p) \quad (2-8)$$

$$- T_w'(t) (1 - \rho A_E L) + T_w'(t) \rho A_E L p'(t)/(\gamma p)]$$

which is the modulated transmission measurement. We assume, subject to later discussion, that $T_w'(t)$ has no significant frequency components above, say 100 Hz, whereas the primary

variation of $p'(t)$ is in a narrow, much higher frequency band (typically near 750 Hz). Furthermore, we ignore the last term, since it contains the product of two small quantities. Then only the first term in Equation 2-8 will contribute significantly to the acoustic bandwidth rms average.

In that case, we have, taking the rms average of Equation 2-8,

$$I_{rms} = I_o T_w \rho A_E L p_{rms} / (\gamma p) \quad (2-9)$$

Now the mass fraction of soot can be determined for the modulating transmission measurement,

$$\rho = \left(\frac{\gamma}{T_w L A_E} \right) \left(\frac{I_{rms}}{I_o} \right) \left(\frac{p}{p_{rms}} \right) \quad (2-10)$$

For jet smoke measurement using a typical transmission cell ($L = 0.1$ m) with visible light ($A_E = 10$ m²/g), this relationship is valid for the full range of smoke emission (0.1-10 mg/m³). The optical density in this case will be small ($\rho A_E L \leq 0.1$).

The smoke mass concentration measurement by modulated transmission is independent of the smoke particle size distribution function for smoke particles of 0.1 μ m diameter and below. This is because the light scattering for smoke is negligible in the Rayleigh regime (diameter < 0.1 μ m for $\lambda = 500$ nm) and the mass specific absorption coefficient is not a function of diameter. For negligible scattering (a very good approximation for smoke), the specific extinction coefficient is¹²

$$A_E \cong A_A = - \frac{6\pi}{\rho_c \lambda} \text{Im} \left[\frac{m^2 - 1}{m^2 + 2} \right] \quad (2-11)$$

where A_A is the specific absorption coefficient (m²/g), ρ_c is the carbon particle density (~ 1 g/cm³), and m is the complex index of refraction for the carbon particle.

As reported by Roessler and Faxvog,¹² the extinction coefficient for soot at visible wavelengths will vary 20% depending on the combustion device. These variations are traced to the extinction coefficient dependence on particle size distribution, index of refraction, particle shape, and organic fraction, which all depend on the specific combustion process.

In practical direct transmission measurements, the cell is first filled with a non-absorbing gas and the transmitted light power is measured (Equation 2-1),

$$I_N = I_o T_w \quad (2-12)$$

Now the transmitted power, I , is measured with the soot present, and the density is given by,

$$\rho = \frac{1}{A_E L} \ln \left(\frac{I_N}{I} \right) \quad (2-13)$$

The difficulty in direct transmission measurements can be seen when this is approximated as,

$$\rho \cong \frac{1}{A_E L} \left(\frac{I_N - I}{I_N} \right) \quad (2-14)$$

In the direct transmission measurement, the soot density depends on the difference of two measured quantities. Since these quantities are nearly equal, when the extinction is small, they must be determined with high precision to yield even a moderately accurate density. On the other hand, the modulated transmission measurement, Equation 2-10, depends directly on the magnitudes of individual quantities, and thus yields density values as accurate as the measurements; this is the primary advantage of the technique.

2.1.3 Experimental Setup

A modulated transmission cell was constructed as shown in Figure 2-2. The cell was made of two brass cylinders (each about 470 mm in length with an inside diameter of 102 mm) separated by the speaker. One side of the cell was used to measure the sample and the other as a speaker resonator. The resonator could be tuned to maximize the acoustic resonance in the sample cell.

The cell walls were of brass material (6.3 mm thick) to minimize the sympathetic vibration of the cylinder walls. Quartz windows (37 mm diameter, 3 mm thick) were placed in the center of the sample cell to pass the light beam. The optical path (L) for the measurements is 100 mm. The smoke sample passed through tube fittings (5 mm ID) on the cylinder walls (Figure 2-2). The microphone was mounted on the center of the end plate on the sample cell.

A schematic of the optical setup and detection electronics is shown in Figure 2-3, and a photograph of the system is shown in Figure 2-4. A microscope illuminator tungsten lamp is powered by a stable dc power supply (7 V, 2.8 A). A tungsten light source is preferred over other light sources (such as lasers and arc lamps) because the tungsten lamp has a very constant light output. The rms magnitude of the modulated transmission signal can be as small as 10^{-6} of the dc light level, and small fluctuations of the light source can limit detection of this small signal. Plasma-generated light sources such as lasers and arc-lamps are inherently noisy light generators.

The lamp light output (25 mm diameter) was filtered by a blue color filter (Corning #5433), passed through the sample cell, and focused to a 10 mm diameter beam by a 75 mm focal length lens onto a silicon photodiode (EG&G model HUV-1100BQ, 1 M Ω feedback resistor, 2.5 mm dia. active area). The photodiode signal was amplified and filtered by a band-pass filter at the speaker frequency. A lock-in amplifier, which was referenced to the speaker drive frequency detected the modulated transmission signal (I_{rms}). The dc level of the photodiode output was monitored by a voltmeter to determine the light intensity (I_0).

The speaker (8 Ω , 4 in. diameter) was driven at a constant frequency (750 Hz) by a signal generator coupled to an audio amplifier. The acoustic frequency at 750 Hz produced an axial acoustic resonance in the cylinder with a maximum pressure oscillation at the light beam loca-

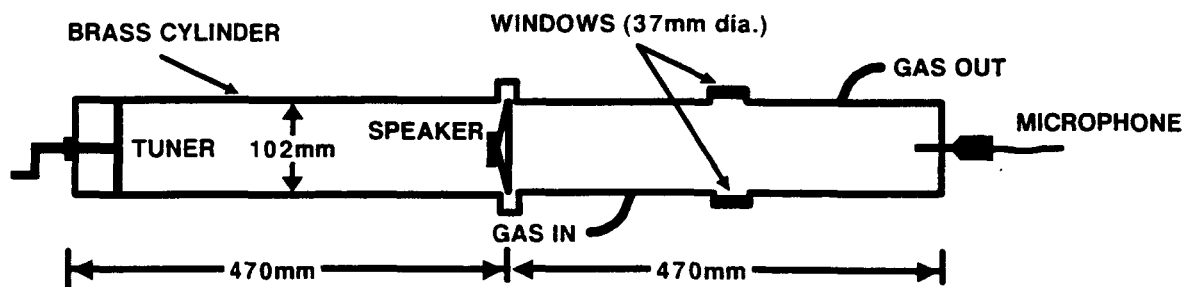


Figure 2-2. Modulated transmission cell

ORIGINAL PAGE IS
OF POOR QUALITY

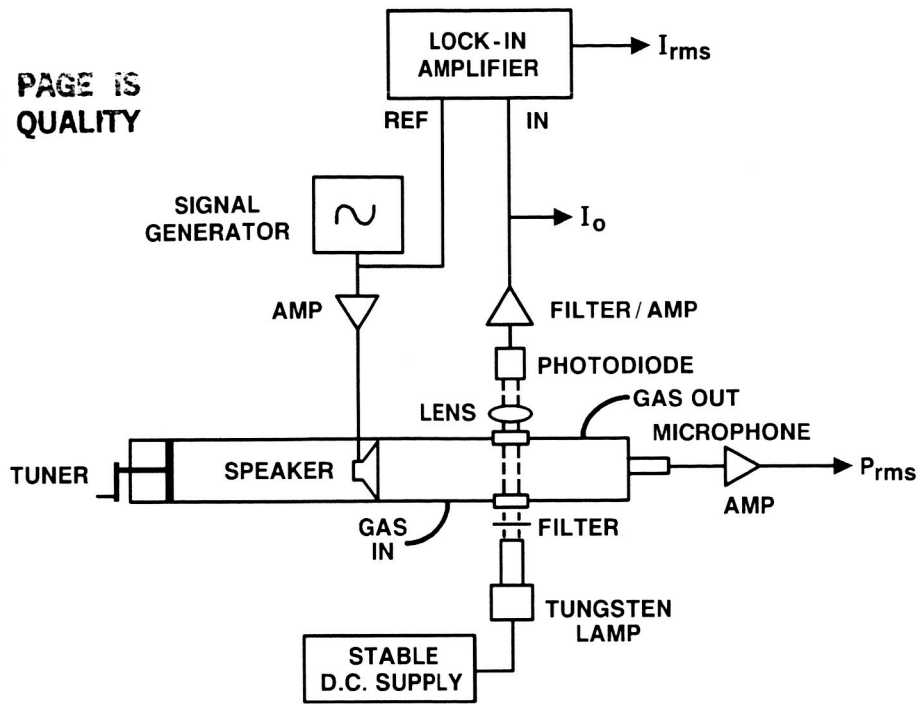


Figure 2-3. Modulated transmission optical setup and detection electronics

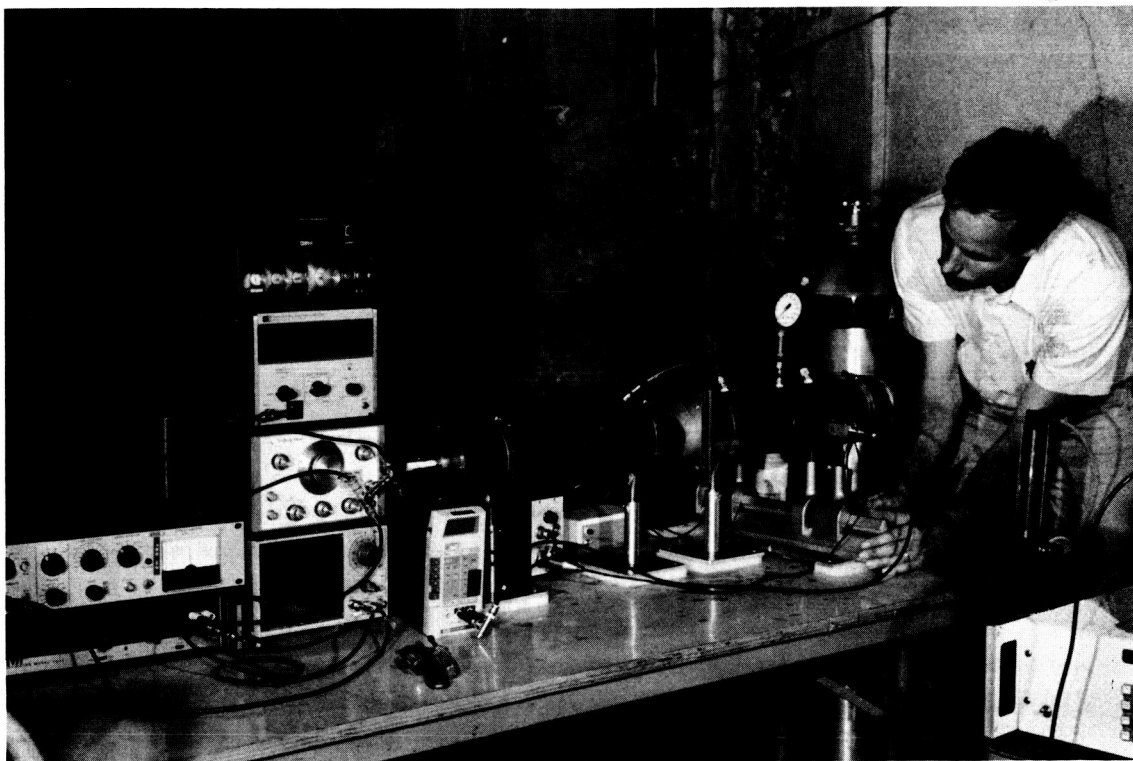


Figure 2-4. Modulated transmission system

tion. Other resonances were tried but the 750 Hz resonance gave the maximum pressure oscillation and thus the maximum modulated transmission signal. The 750 Hz resonance produces an acoustic pressure oscillation in the beam which has an rms level of about $p_{rms}/p = 0.15\%$ or about 140 db. The signal from the microphone (B&K Model 4135) was amplified by a B&K Model 2618 amplifier and recorded by an rms voltmeter to determine p_{rms} . The microphone was calibrated by a piston phone, which gave 3.48 mV/pascal.

2.1.4 Nitrogen Dioxide Measurements

Small amounts of NO₂ were used to simulate smoke absorption and test the sensitivity of the MODTRAN technique. Known concentrations of NO₂ gas diluted in nitrogen were passed through the cell, and both modulated transmission and direct transmission techniques were used to measure the extinction coefficient of NO₂. (A_{NO_2} was calculated from Equations 2-10 and 2-13.) The results for the two different calibration bottles shown in Table 2-1 gave values of A_{NO_2} that compared within less than 2%. Levels in the calibration bottles are shown since NO₂ levels in the calibration bottles may change slightly with time. The slight variation in the measured value of A_{NO_2} is probably due to uncertainties in the NO₂ concentrations in the bottles. In all experiments with NO₂, reduced levels of NO₂ are obtained from a single calibration bottle which is diluted with nitrogen using calibrated sonic orifices so that uncertainty in the NO₂ levels in the calibration bottles does not affect the linearity of the results.

The average extinction coefficient from Table 2-1 is 0.42 m²/g. Thus 1 mg/m³ of smoke will be equivalent to the following density of NO₂:

$$\rho_{NO_2} = \frac{\rho A_E}{A_{NO_2}} = (1 \text{ mg/m}^3) \frac{10 \text{ m}^2/\text{g}}{0.42 \text{ m}^2/\text{g}} = 24 \text{ mg/m}^3 \quad (2-15)$$

At one atmosphere pressure and a temperature of 21 °C, this is equivalent to 12.5 ppm of NO₂.

Next, the sensitivity limits of modulated transmission were tested by measuring small amounts of NO₂ diluted in nitrogen, which simulated low levels of smoke. In this test, NO₂ from two calibration bottles (200 ppm and 207 ppm) was diluted with additional nitrogen using calibrated critical flow orifices. Diluted NO₂ samples down to 25 ppm of NO₂ (equivalent to 2 mg/m³ of smoke) were tested, and the results are shown in Figure 2-5. The ideal system response is given by the straight line through the origin. The values at 200 ppm and 207 ppm are the system calibration points, which, by definition, fall on the ideal line.

Table 2-1
Nitrogen Dioxide Measurements

NO ₂ Calibration Gas (ppm)	Measurement Technique	A_{NO_2} (m ² /g)	Difference (%)
200	Direct Transmission	0.414	0.5
	MODTRAN	0.416	
207	Direct Transmission	0.421	1.4
	MODTRAN	0.427	

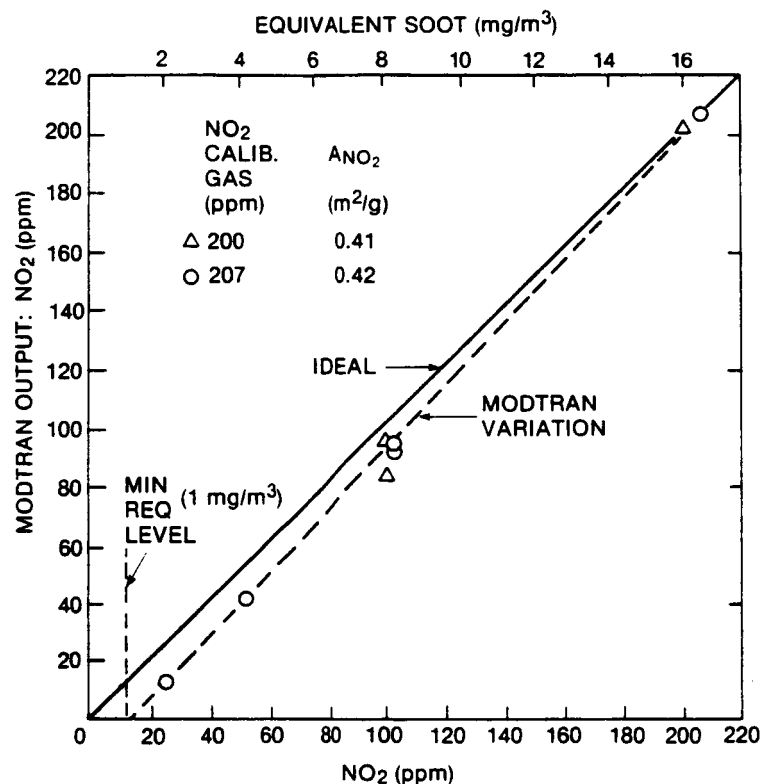


Figure 2-5. Modulated transmission signal from diluted samples of NO₂ in nitrogen

The signal response is linear and shows a good signal-to-noise ratio down to about 35 ppm of NO₂, which is equivalent to 3 mg/m³. This is about three times the lower sensitivity limit given in the "General Smoke Meter Requirements" given in Appendix A.

2.1.5 Smoke Measurement

Measuring smoke from a smoke generator, the modulated transmission technique was compared to two other instruments: a standard soiled tape meter^{4,5} and a tapered element oscillating microbalance^{13,14} (TEOM, a commercially available instrument). The smoke generator was built after a design by Lee and Mulholland.¹⁵ Smoke from the soot generator was alternatively measured in all three instruments as shown in Figure 2-6.

For the soiled tape meter, the reflectance of each spot was determined by a reflectometer and the smoke number determined according to Aerospace Recommended Practice 1179A.⁵ The smoke numbers were then converted to smoke density using the correlation determined by Shaffernocker and Stanforth.⁴ During the test the smoke numbers and smoke densities ranged from 5 to 88 and 0.5 to 127 mg/m³, respectively.

The TEOM instrument collects the soot in a filter element mounted on the end of a hollow vibrating tube, where the vibration frequency gives a real-time measure of the collected particulate mass. The technique is described in detail by Wang et al.¹³ The instrument records the collected soot mass, Δm , and the soot density is given by

$$\rho (\text{mg/m}^3) = \frac{\Delta m (\mu\text{g})}{t (\text{min}) Q (\text{l/min})} \quad (2-16)$$

where t is the collection time and Q is the volumetric flow rate. The values of Δm and t were determined from the strip chart output of the TEOM. Only a few measurements were

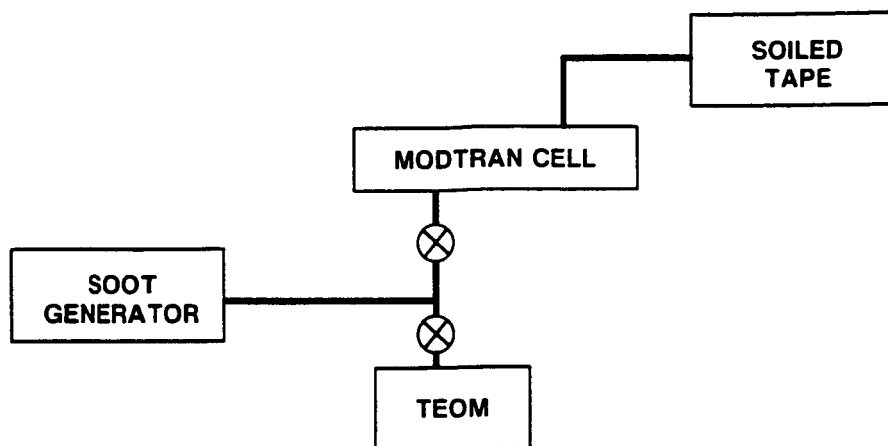


Figure 2-6. Flow schematic of modulated transmission test measuring smoke

made with the TEOM instrument because it was difficult to get a stable output, particularly after a new filter was installed.

The burner did not function as a stable source normally used to calibrate instruments. The smoke output of the burner was difficult to adjust and would often vary uncontrollably throughout the experimental run. After 30 minutes the burner would become contaminated with smoke deposits and need to be cleaned. The measurements from the different instruments could not be taken simultaneously but were taken in rapid succession (usually within a minute of each other) to attempt to sample the same level of smoke given off by the burner. The MODTRAN cell was cleaned before each experiment. The smoke density measurements are given in Figures 2-7, 2-8, and 2-9.

In the first test (Figure 2-7) the MODTRAN and soiled tape instruments were compared for smoke levels 2 to 14 mg/m^3 . Other than the very high smoke value for the soiled tape at 16 mg/m^3 , all the values seem to agree within $\pm 10\%$ of each other. The value for A_E of 10 m^2/g (which is typical of literature values in the visible range,¹² which vary between 8 to 10 m^2/g) was used in all these results and seemed to give good correspondence between the MODTRAN and soiled tape instruments.

In the second test (Figure 2-8) a comparison of the TEOM and MODTRAN instruments was made at high smoke levels (up to 88 mg/m^3). The TEOM instrument did not operate very well at these levels because the filter became choked with soot very quickly. The manufacturer indicates that a filter pressure drop of 15 in. Hg or greater is unacceptable. After installing a clean filter in the TEOM, a pressure drop of 15 in. Hg was reached in as little time as 3 minutes at these high smoke levels. As the pressure drop built up, there seemed to be a rapid decrease in the TEOM output until at a pressure of 15 in. Hg pressure, the signal was as much as 75% too low. When starting with a clean filter at these high smoke levels ($> 70 \text{ mg}/\text{m}^3$), only the first one or two TEOM readings seemed to agree with the MODTRAN output.

All three instruments are compared in the last test in Figure 2-9. For the measurements around 3-4 mg/m^3 , all the measurements are within $\pm 30\%$ or $\pm 1 \text{ mg}/\text{m}^3$. As the smoke level was increased, the results showed more scatter up to $\pm 50\%$. It is not clear whether most of the scatter is due to fluctuation in the soot source or measurement uncertainty.

The results, including data not shown in Figures 2-7 to 2-9, are summarized in Table 2-2, where the smoke levels measured by the MODTRAN and TEOM instruments are compared

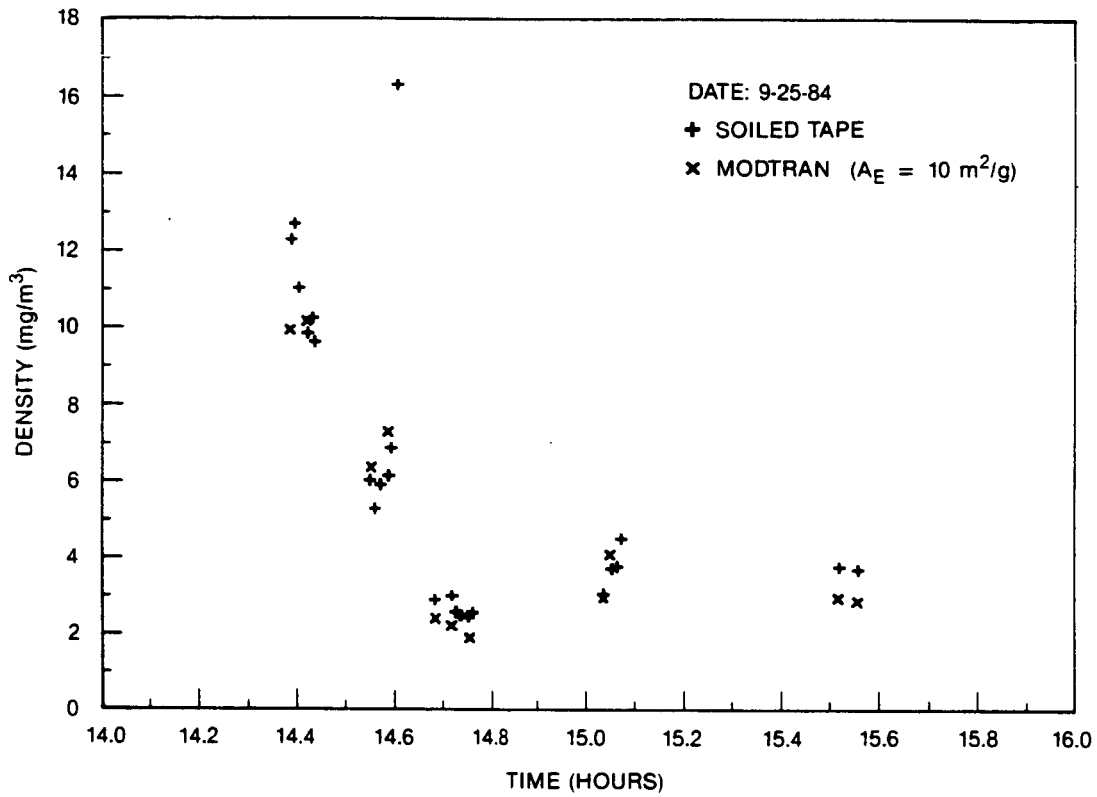


Figure 2-7. Comparison of the modulated transmission and soiled tape instruments measuring smoke

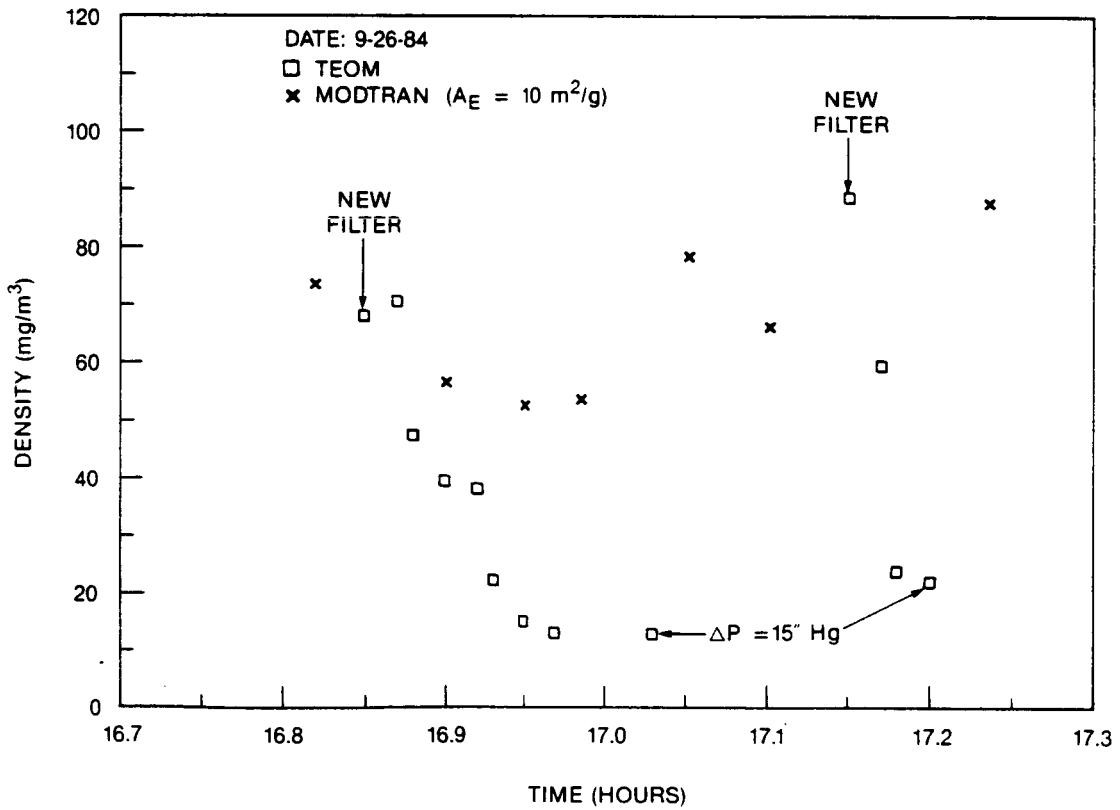


Figure 2-8. Comparison of the modulated transmission and TEOM instruments measuring smoke

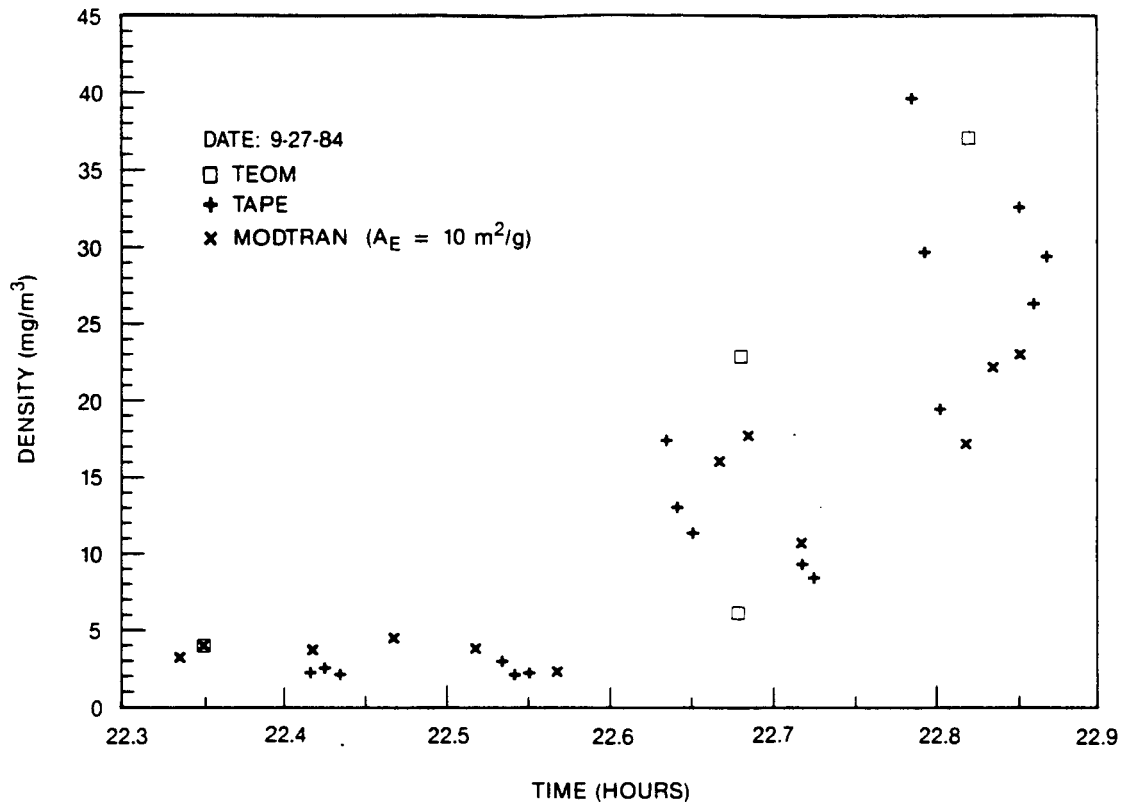


Figure 2-9. Comparison of the modulated transmission, soiled tape, and TEOM instruments measuring smoke

Table 2-2
Comparison of MODTRAN and TEOM Instruments
To the Soiled Tape Smoke Meter

Smoke Density (mg/m^3)	Smoke No.	MODTRAN		TEOM	
		Low (%)	High (%)	Low (%)	High (%)
0.5-2	7-20	-60	-50	-	-
		-50	-50	-	-
2-4	20-31	-25	0	-	-
		0	50	-	-
		-50	-10	-40	10
4-10	31-47	-20	10	-	-
		-10	10	-50	-30
		-50	30	-20	1
10-20	47-59	-20	0	-	-
		-10	40	40	80
20-50	59-74	-50	10	-	-
		-30	-20	-20	20
50-100	74-85	-50	0	-	-

to the standard soiled tape smoke meter. These results are based on very few points (especially for the TEOM instrument) and are difficult to interpret because the smoke source fluctuated during the runs. However, a few trends can be seen. In the lower range (0.5-2.0 mg/m³), the MODTRAN instrument read low. There were mixed results from 2 to 4 mg/m³ (smoke numbers 20-31). The MODTRAN instrument generally agreed with the soiled tape meter in the range 4-20 mg/m³ (smoke numbers 31-60). In the high range (20-100 mg/m³) the MODTRAN signal is low sometimes, for a number of possible reasons:

1. The MODTRAN signal could be lower due to window contamination, which reduces the window transmission.
2. There could be significant agglomeration in the cell at these high soot levels to form larger sized particles. The specific absorption coefficient of soot decreases for larger particle sizes (greater than about 0.2 μ m) according to MIE scattering calculations (see Figure 4 of Reference 3).
3. The soiled tape measurement is too high because of inaccuracies at high soot levels where the reflectance is nearly zero and difficult to measure reliably.

Only a few points were measured with the TEOM because of difficulties in getting the instrument to stabilize. The only firm conclusion is that sampling of undiluted high-level smoke (greater than 50 mg/m³) is difficult as the filter is rapidly choked with soot, resulting in readings as much as 75% low.

2.1.6 Evaluation

The major problem with the modulated transmission technique is the lack of sensitivity at the low levels of smoke. The lower limit of sensitivity is determined to be about 3 mg/m³ from both the NO₂ and smoke measurements. This is about 30 times higher than the smoke meter requirements (Appendix A).

Various improvements, such as multi-beam pass and alternative cell designs (and alternative acoustic resonances) were considered to increase the signal level. In addition, the cell could be constructed of lead to minimize window vibrations and increase the signal-to-noise ratio. However, these improvements are unlikely to achieve the factor of 30 needed for a lowered sensitivity limit of 0.1 mg/m³.

Because of window contamination, the MODTRAN instrument measured lower than expected signals for high levels of smoke (20 to 100 mg/m³). These high levels are seldom encountered in jet engine exhausts and above the smoke density range given in Appendix A. However, the MODTRAN cell should be designed to minimize contamination of the windows by soot.

Although the MODTRAN optical signal has good frequency response (liters per second), the cell volume of the MODTRAN system is large (3.8 liters) and will certainly limit the ultimate time response of the instrument. A sample frequency of liters per second is desirable (Appendix A). This would require a sample flow rate of about 4 liters/second. This smoke sample flow rate is about 10 times higher than current smoke meters. The standard soiled tape meter has a sample flow rate of only 0.2 liter/second. Thus, a reduction of the MODTRAN cell size is desirable to reduce the sample flow rate requirements and improve the frequency response. However, a reduction of the cell size would only increase the sensitivity problems as the optical path length would be reduced.

2.2 PHOTOTHERMAL DEFLECTION SPECTROSCOPY (PDS)

2.2.1 General Description

A recently developed technique that was not considered in the initial survey of smoke meter techniques⁸ does hold promise of detection down to 0.1 mg/m^3 of smoke. A technique called "photothermal deflection spectroscopy" (PDS) has been demonstrated in gases measuring ethylene¹⁶ to an absorption level of 10^{-5} m^{-1} , which is 100 times more sensitive than needed for the present smoke instrument. For 0.1 mg/m^3 , the absorption for soot in the visible ($\lambda = 0.5 \mu\text{m}$) is

$$\rho A_A = (0.1 \text{ mg/m}^3)(10 \text{ m}^2/\text{g}) = 10^{-3} \text{ m}^{-1} , \quad (2-17)$$

which should be easily measurable with PDS since it is 100 times larger than the previously demonstrated sensitivity limit.

The PDS technique is based on heating a probe laser beam with a modulated pump beam (see Figure 2-10). The small diameter probe beam crosses the larger pump beam at a small angle. The higher energy pump beam is absorbed by the smoke, which heats the gas and deflects the probe beam. The gas is alternately heated and allowed to cool by modulating the pump beam, producing an oscillating deflection of the probe beam that is easily detected by a position sensor and a lock-in amplifier. The deflection signal is proportional to the optical absorption of the smoke, which is closely related to the smoke density.

The PDS technique has been demonstrated for absorption measurement in gases (ethylene,^{16,17} propane,¹⁸ nitrogen dioxide¹⁹ and hydroxyl radicals²⁰) liquids,²¹ solids,²² and thin films.²² The gas absorption measurements have been reported for both static conditions^{16,18} and flowing conditions (i.e., jets,¹⁷ flat flame burners,¹⁹ and premixed flames²⁰).

2.2.2 Theoretical Principles

A schematic of the method for gas or smoke analysis is shown in Figure 2-11. The output beam of an argon-ion laser (all visible lines, 1.3 mm diameter) crosses a He-Ne probe beam (632.8 nm, 0.9 mm diameter) in the measurement zone at a small angle, θ . The cross-sections of the intersection of the two beams is shown in Figure 2-10. The argon-ion pump laser is modulated by a mechanical chopper. The smoke particles absorb the light and the gas in the pump beam is heated. The temperature gradient produced by the heating induces an index of refraction gradient that deflects the probe beam at the modulation frequency. The deflection of the probe beam is detected by a position sensor (photodiode bi-cell). Both a double-density flint prism and a narrow band (1 nm) interference filter are used to reject any light from the pump beam. The output of the bi-cell is amplified and sensed by a lock-in

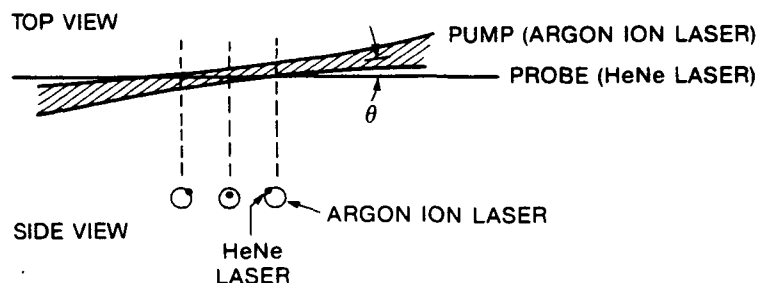


Figure 2-10. Photothermal deflection spectroscopy (PDS) beam crossing schematic

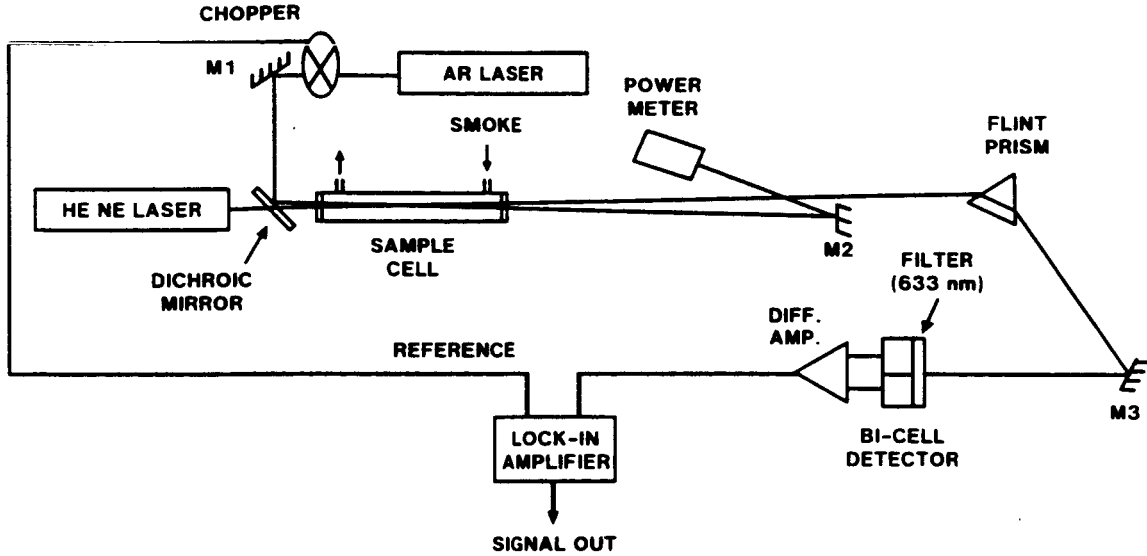


Figure 2-11. PDS optical setup and detection electronics

amplifier. The lock-in amplifier rejects noise signals that are not at the frequency of the modulated pump laser.

The deflection angle (radians) of the beam for low modulation frequencies where the thermal diffusion length is larger than the pump beam radius is²¹

$$\phi = C \frac{dn}{dT} \frac{I_0}{k\pi^2 x_0} \left[1 - e^{-b_a L} \right] \left[1 - e^{-x_0^2/a^2} \right] \quad (2-18)$$

where n is the index of refraction, I_0 is the laser power (watts), k is the thermal conductivity of the gas (w/m-K), x_0 is the minimum separation of the probe and pump beams, b_a is the optical absorption (m^{-1}), L is the beam crossing length (m), a is the radius of the pump beam (m) and C is a constant resulting from the small beam crossing angle ($C \approx 1$). (A more rigorous expression for PDS deflection in a co-linear system (small crossing angle) is given by Jackson et al.²³) For smoke, the optical absorption will be small ($b_a L \ll 1$), giving

$$1 - e^{-b_a L} \cong b_a L = \rho A_A L \quad (2-19)$$

where ρ is the smoke density (mg/m^3) and A_A is the mass specific absorption of smoke (m^2/g). The probe laser is positioned at the location of maximum signal ($x_0 = a$) and the deflection angle (radians) is given by

$$\phi = 0.6321 \cdot C \frac{dn}{dT} \frac{\rho A_A L I_0}{k\pi^2 x_0} \quad (2-20)$$

The actual deflection on the detector will be

$$\Delta x = R\phi \quad (2-21)$$

where R is the distance from the deflection point to the detector.

The index of refraction variation with temperature is given by Gladstone and Dale's empirical law.²⁴

$$(n-1)/\rho = \text{constant} \quad (2-22)$$

or

$$\frac{(n-1)}{\rho} = \frac{(n_o-1)}{\rho_o} \quad (2-23)$$

where n_o and ρ_o are the index of refraction and gas density at reference conditions. Solving Equation 2-23 for n and differentiating with respect to temperature, we have

$$\frac{dn}{dT} = - \frac{T_o}{T^2} (n_o-1) \quad (2-24)$$

For light at $\lambda = 0.6$ propagating in the atmosphere at $T_o = 288$ K (15 °C), the index of refraction is $n_o = 1.000276$. Experiments will be typically performed at room temperature, $T = 294$ K (21 °C), and the differential is,

$$\frac{dn}{dT} = 9.2 \times 10^{-7} \text{ K}^{-1} \quad (2-25)$$

For a PDS instrument detecting smoke, typical parameters will be:

$$\begin{aligned} C &= 1.0 \\ I_o &= 1.0 \text{ W} \\ x_o &= 0.65 \text{ mm} \\ L &= 0.01 \text{ m} \\ k &= 0.026 \text{ w/m-K} \\ A_A &= 10 \text{ m}^2/\text{g} \end{aligned}$$

At the lower limit of smoke detection, $\rho = 0.1 \text{ mg/m}^3$, the minimum deflection angle will be

$$\phi \cong 3 \times 10^{-8} \text{ radians}$$

or for $R = 1$ meter the deflection will be,

$$\Delta x \cong 30 \text{ nm}$$

Detection of this signal is easily attainable since the sensitivity limit of bi-cell detectors²⁵ is listed as ± 0.1 nm.

The temperature rise due to the light absorption is slight. For the typical PDS system described above, the calculated temperature rise ranges from about 0.01 K to 1 K for smoke densities ranging from 0.1 to 12 mg/m^3 .

It is desirable to operate at the highest modulation frequency possible to give the best time response for the smoke meter. The highest modulation frequency will be when $l_d \approx a$ where l_d is the thermal diffusion length at the modulation frequency. At high modulation frequencies ($l_d < a$) the deflection signal decreases with increasing frequency, which is undesirable ($\Delta x \approx 1/f$, where f is the modulation frequency²¹).

The thermal diffusion length is related to the modulation frequency by,

$$f = \alpha/l_d^2 \quad (2-26)$$

where α is the thermal diffusivity (m^2/s). For a pump beam with a 0.65 mm radius in air ($\alpha = 2.15 \times 10^{-5} \text{ m}^2/\text{s}$), the highest modulation frequency without loss of signal will be about 50 Hz (where $l_d \approx a = 0.65 \text{ mm}$). For smoke measurement, the maximum modulation frequency will be lower because the heated smoke particles cool more slowly than the gas.

The PDS system was first tested measuring NO_2 to simulate smoke absorption. The average extinction coefficient of NO_2 at the argon-ion visible wavelengths (476.5-514.5 nm) is about $0.34 \text{ m}^2/\text{g}$.²⁶ Thus, $1 \text{ mg}/\text{m}^3$ of smoke will be equivalent to the following density of NO_2 ,

$$\rho_{\text{NO}_2} = \frac{\rho A_A}{A_{\text{NO}_2}} = (1 \text{ mg}/\text{m}^3) \frac{10 \text{ m}^2/\text{g}}{0.34 \text{ m}^2/\text{g}} = 29 \text{ mg}/\text{m}^3 \quad (2-28)$$

At one atmosphere pressure and a temperature of 21°C , this is equivalent to 16 ppm of NO_2 .

2.2.3 Experimental Setup

The optical setup used in the tests is shown in Figure 2-11. The argon-ion pump beam (1.3 mm diameter, 1-5 W, all visible lines, 476.5-514.5 nm) is combined with a helium-neon probe beam (0.9 mm, 5-15 mW, 632 nm) with a dichroic mirror, and the two beams cross in the sample cell at an angle of $\approx 0.5^\circ$. The minimum beam separation (see Figure 2-10) is equal to the pump beam radius (0.65 mm) that gives the maximum deflection signal. The sample cell is a cylinder (305 mm long by 12.7 mm inside diameter) made of black anodized aluminum with two window flats on each end. The sample gas enters and exits the cell through tube fittings (5 mm ID) mounted on the sidewall near each end. Care is taken that the pump and probe beams do not intersect on the windows to avoid spurious beam deflections due to heating of window contaminants. The small cell volume (39 cc) gives fast sampling of the smoke at moderate flow rates (1 volume exchange per second at 2.4 liters/min). (The standard soiled tape meter operates at 12 liters/min sample flow.)

The pump beam is modulated by a chopper at a fixed frequency (750 Hz for NO_2 measurements and 48 Hz for smoke measurements). The modulated pump beam power is monitored continuously by a power meter. After passing through the cell, the helium-neon probe beam is deflected by a double-density flint prism and directed by a mirror onto a bi-cell detector (EG&G Model UV-140BQ-2), which is placed 1.7 m from the beam crossing point. The flint prism disperses any residual argon-ion light away from the bi-cell detector. An interference filter (1 nm band-pass) mounted on the bi-cell detector eliminates any stray light. The bi-cell position detector signal is differentially amplified, passed through a band-pass filter, and detected by a lock-in analyzer referenced to the chopper frequency. The magnitude of the lock-in output is linearly proportional to the absorber concentration (either smoke or NO_2). A photograph of the PDS smoke measurement system is shown in Figure 2-12.

2.2.4 Nitrogen Dioxide Measurements

The PDS system was analyzed and calibrated using NO_2 (370 ppm) simulating smoke. The detected signal level from NO_2 as a function of the laser power is shown in Figures 2-13 and 2-14. The laser power shown is the average power of the modulated argon beam exiting the sample cell. For example, at a laser power setting of 4 W continuous light, the average power of the modulated light exiting the sample cell is 1250 mW. All the NO_2 measurements are at a modulation frequency of 750 Hz and a time constant ranging from 1 to 3 seconds for the lock-in amplifier. In Figure 2-13, the signal shows good linearity with laser power for equivalent smoke levels of 2 to 23 mg/m^3 (16 ppm of NO_2 is equivalent to $1 \text{ mg}/\text{m}^3$ of smoke). Figure 2-14 shows the lower range of equivalent smoke from 0.2 to 1.5 mg/m^3 . Even at $0.2 \text{ mg}/\text{m}^3$ of equivalent smoke, the signal shows good linearity and signal-to-noise ratio. Repeated measurements at this level showed only a $\pm 5\%$ variation.

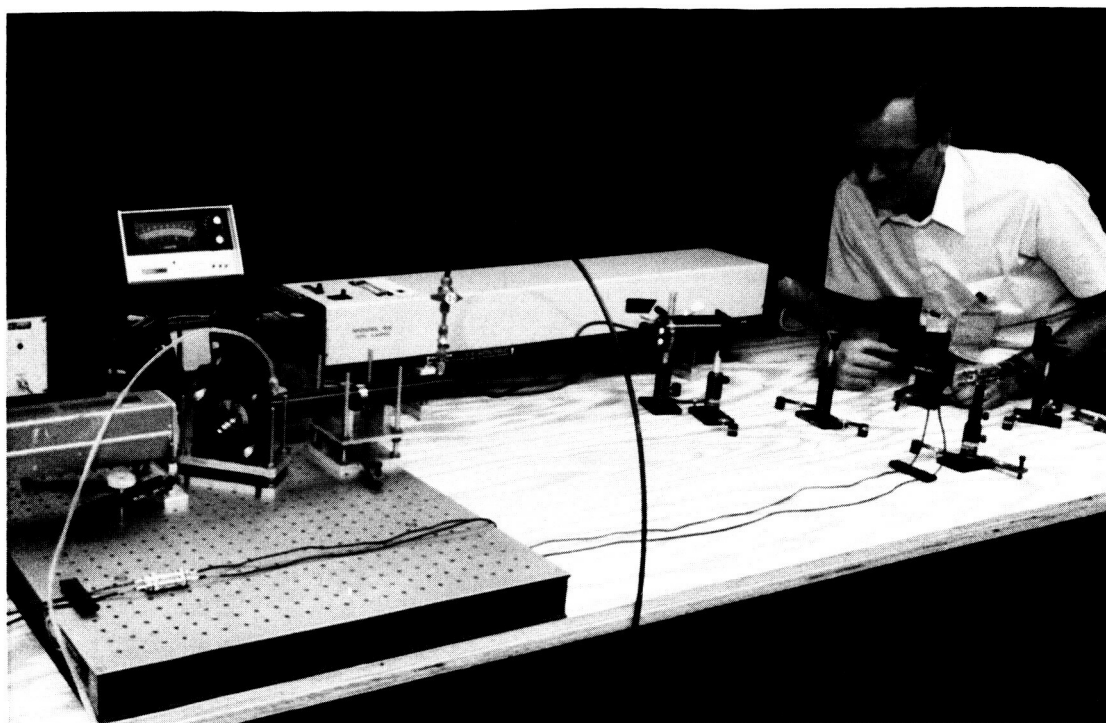


Figure 2-12. PDS system

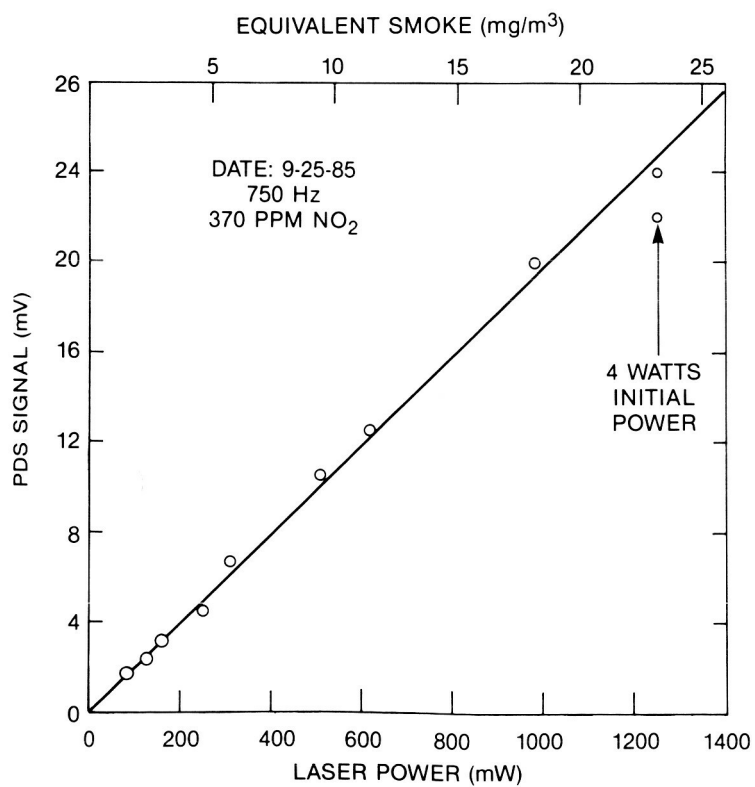


Figure 2-13. PDS signal variation at high laser power

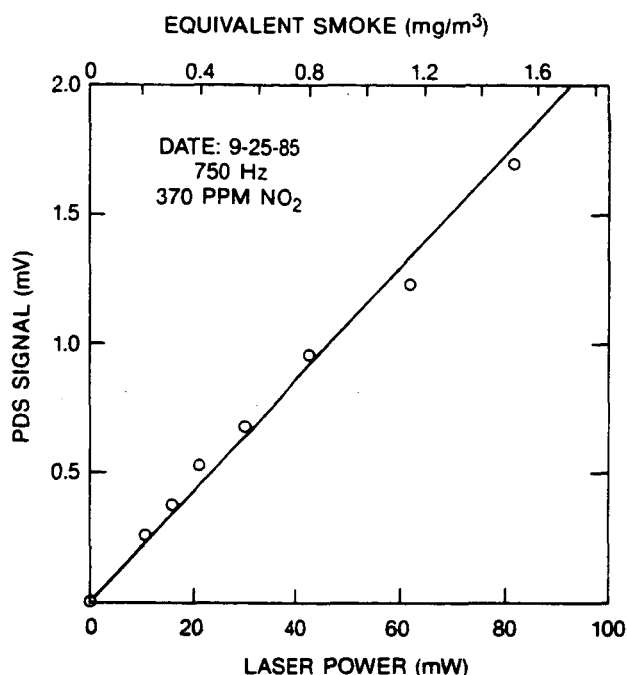


Figure 2-14. PDS signal variation at low laser power

The PDS system was tested with very low levels of NO_2 to establish its sensitivity. As shown in Figure 2-15, the PDS signal showed good linearity and excellent sensitivity down to 3.5 ppm of NO_2 , which is equivalent to about 0.2 mg/m^3 of smoke. In this measurement, the noise level was very low—only 0.01 mV. Thus for signal-to-noise levels of 10 and 3, the lowered bounds of sensitivity for smoke are $25 \text{ } \mu\text{g/m}^3$ and $8 \text{ } \mu\text{g/m}^3$ respectively. At $10 \text{ } \mu\text{g/m}^3$ of smoke, the light absorption is only 0.01% per meter ($10^{-4} \%$ per cm). The effective sample volume is about 20 cm long, giving a total absorption of 0.002%. Previously, the MODTRAN instrument had difficulty measuring 3 mg/m^3 , which is about 3% per meter absorption. Thus the PDS instrument exhibits sensitivity limits that are over 100 times better than the MODTRAN instrument.

The effect of the sample cell flow rate on the PDS signal was measured. For sample flows between 1.5 cc/sec to 100 cc/sec, there was no measured effect of the flow rate. However, when the flow was shut off so that the NO_2 -laden gas was stationary, the PDS signal decreased about 15%. Since the cell was completely leak tight, this decrease is not due to dilution of the sample by leakage of outside air. The flowing sample probably enhances the signal slightly by increasing the heat convection during the cooling cycle.

2.2.5 Smoke Measurement

The PDS instrument was tested measuring smoke and compared to the TEOM¹³ and the standard soiled tape instruments.⁴ As before with the MODTRAN instrument a burner modeled after a design by Lee and Mulholland¹⁵ was used to produce smoke. Also a differential mobility analyzer (DMA) measured the smoke particle size produced by the smoke generator. The flow system is shown in Figure 2-16. In all comparisons the PDS signal was recording simultaneously with each instrument. Because the smoke output from the smoke generator was erratic, a 30 second time response was used for the PDS electronics. The smoke sample flow rate was 3 liters/min except when using the DMA, which could tolerate a flow rate of only 0.6 liter/min. At 3 liters/min, the smoke sample in the cell is purged at a frequency of 1.3 Hz. The particle size distribution as measured by the DMA is given in Figure 2-17. The median smoke particle size is $0.04 \text{ } \mu\text{m}$ diameter (50% of the

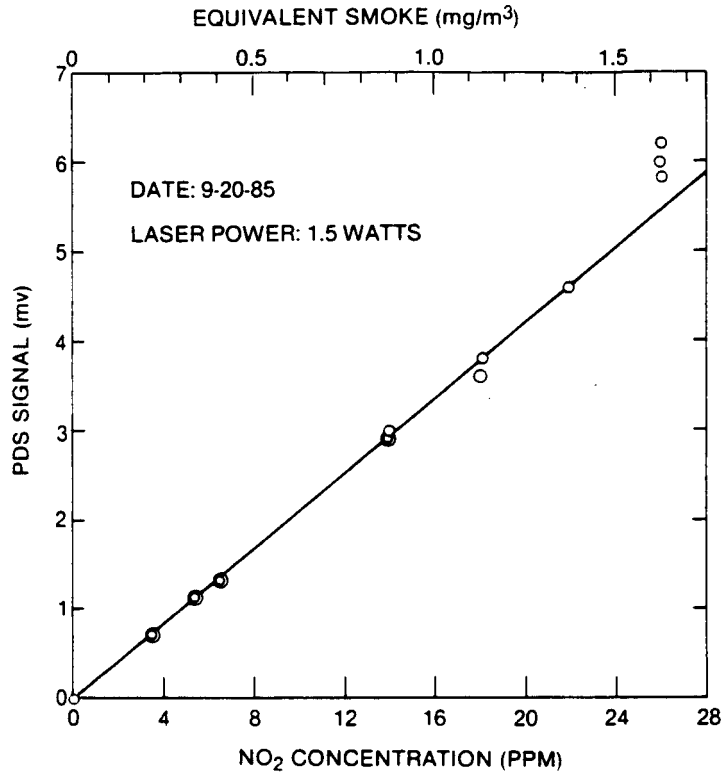


Figure 2-15. PDS signal variation from diluted samples of NO₂

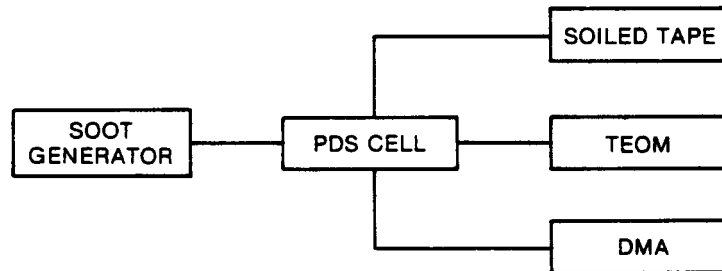


Figure 2-16. Flow schematic of PDS test measuring smoke

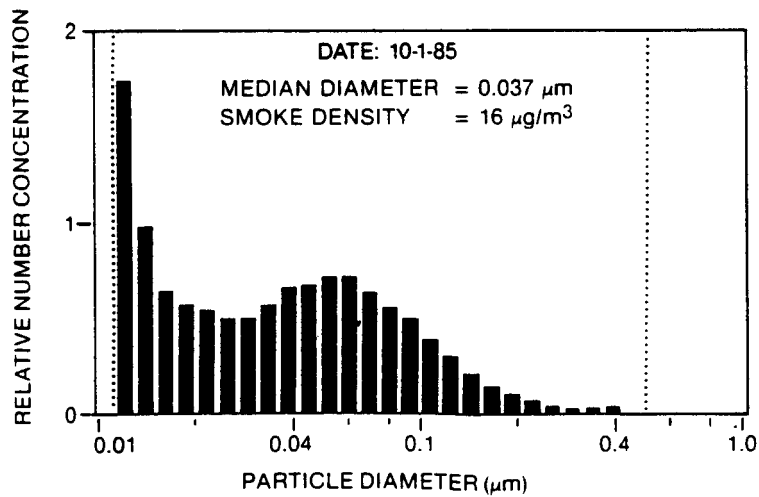


Figure 2-17. Particle size distribution of the smoke generator output as measured by a differential mobility analyzer

smoke particles are below this size). At this smoke particle size, the coefficient A_A and therefore the PDS signal are independent of particle size (see Equations 2-11 and 2-20).

The smoke measurement test of the PDS system was performed in a laboratory where a standard optical bench was unavailable. A crude optical table was constructed from two 8 ft \times 4 ft \times $\frac{3}{4}$ in. pieces of plywood, which were screwed together and placed on a laboratory bench. This configuration was not as rigid as the optical tables used in the past. Because the table was not rigid, the probe beam gradually moved off the center of the bi-cell and had to be re-centered about every half-hour. The dc level of the differential amplifier was constantly monitored on an oscilloscope to make sure that the probe beam was centered. No attempt was made to isolate the table from vibrations. Vibration from a large compressor nearby produced a low-frequency signal on the bi-cell detector that was equivalent to a large smoke signal. However, the lock-in detection easily removed this interference, and the sensitivity of the detection was nearly as good as that obtained under ideal laboratory conditions. For example, the data shown in Figures 2-13 and 2-14 was measured using this wooden optical bench and shows excellent sensitivity. The excellent performance of the PDS system under these hostile conditions suggests that a properly designed PDS meter could be operated in the proximity of a jet engine.

Next the PDS smoke meter was tested with smoke and compared to other instruments (Figure 2-16). The sensitivity of the PDS smoke meter to smoke ranged from 0.04 to 3 mg/m³ per mv of signal depending upon the laser power setting. The dynamic range of the instrument was easily set by increasing or decreasing the laser power. The PDS meter was regularly calibrated with NO₂ to measure the exact system response. The windows became contaminated from smoke and the PDS signal was corrected in the following fashion: the modulated pump laser power exiting the cell was measured with clean windows and monitored continuously throughout the measurements to determine the average power of the argon-ion beam in the cell.

In the first measurement of smoke, the PDS instrument showed a sharply decreased sensitivity to smoke. The signal was about 20 times lower than expected. The lower signal was due to the lower effective thermal diffusivity of smoke. The smoke particles give up the absorbed heat much more slowly than NO₂. In order to increase the PDS signal from the smoke particles, the chopping frequency was lowered from 750 Hz to 48 Hz. The PDS signal increases with decreasing chopping frequency in the high frequency limit where the time it takes heat to diffuse is short compared to the chopping period.²¹ At the lowered frequency of 48 Hz, the PDS meter showed excellent sensitivity to smoke.

Next it was determined that measurable interfering quantities of NO₂ were being produced by the smoke generator. There was a PDS signal corresponding to about 0.3 mg/m³ of smoke when all the smoke was filtered from the smoke generator output. The interfering NO₂ was particularly troublesome at low levels of smoke (less than 1 mg/m³). In order to remove this interfering gas, the air in the burner was replaced with a mixture of 20% oxygen and 80% argon. All the nitrogen-bearing species in the burner were removed precluding the formation of NO₂. Since NO₂ is the only interfering gas, the PDS measurement of smoke could be directly compared to measurements with other instruments.

The comparison of the PDS meter to the soiled tape meter is shown in Figure 2-18 for high smoke levels. For all the PDS smoke measurements, a mass specific absorption coefficient of $A_A = 10 \text{ m}^2/\text{g}$ was used. The smoke generator output was very erratic, which produced an unsteady PDS signal and made averaging of the PDS signal necessary. The soiled tape meter averaged the smoke level over a period of about 2 minutes and the PDS meter was averaged over the same period. The two meters showed good agreement at high

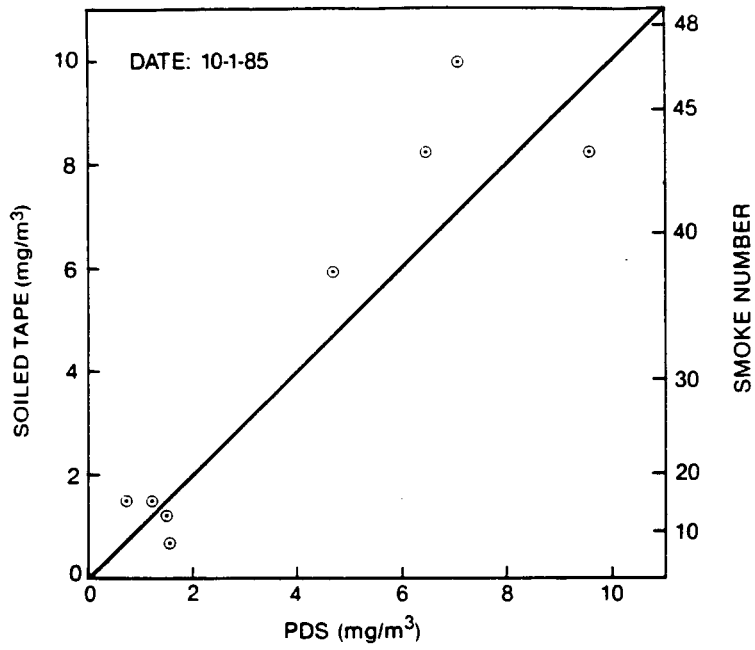


Figure 2-18. Correlation between the PDS and soiled tape instruments for high smoke levels (— ideal correlation)

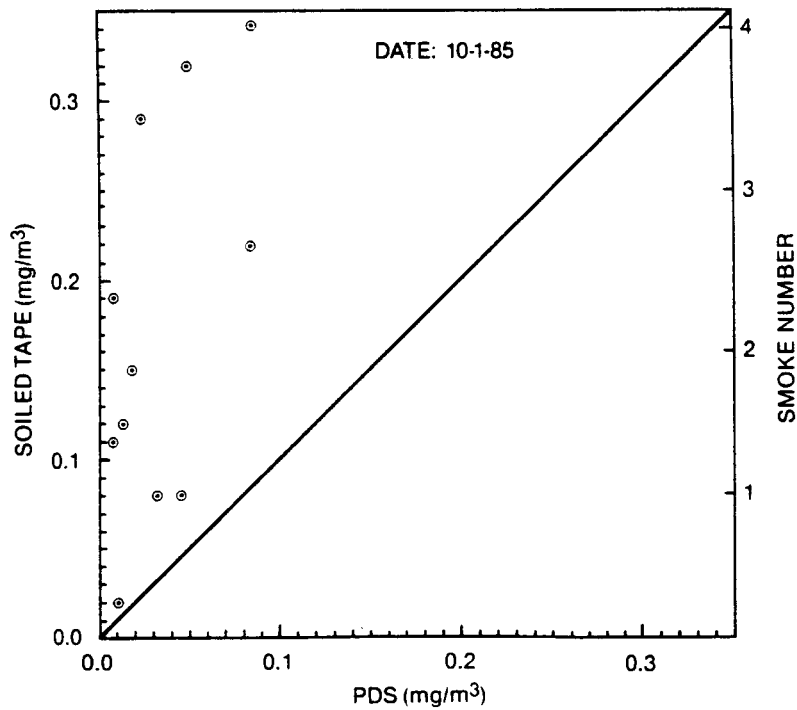


Figure 2-19. Correlation between the PDS and soiled tape instruments for low smoke levels (— ideal correlation)

levels (6 to 10 mg/m³) but at levels below 2 mg/m³, the correspondence was poor. At lower smoke levels (below 2 mg/m³) as shown in Figure 2-19, the soiled tape meter does not give reliable readings. This is consistent with the results of Champagne⁹ who found the soiled tape meter was over 100% uncertain for smoke levels below 0.5 mg/m³.

A time history of the PDS and the TEOM signals for the lower range of smoke levels is shown in Figure 2-20. Both the PDS and TEOM instrument show qualitatively similar signals for smoke levels ranging from 0.3 to 2 mg/m³. At levels below 0.3 mg/m³, the TEOM instrument produces an unsteady signal, as seen in Figure 2-20, when the burner went out at about 5 minutes. The TEOM signal oscillated, showing negative weights as low as -0.4 mg/m³ when the burner extinguished. During the same period, the PDS signal dropped steadily to zero. The PDS meter showed excellent resolution to smoke levels as low as 0.05 mg/m³.

2.2.6 Evaluation

From the NO₂ measurements simulating smoke absorption, the PDS smoke meter demonstrated excellent sensitivity and signal-to-noise ratio down to 200 μg/m³. The excellent signal-to-noise ratio at 200 μg/m³ in the NO₂ data indicate that measurements down to 25 μg/m³ are possible with a signal-to-noise ratio of 10. The NO₂ measurements show excellent linearity from 0.2 to 20 mg/m³.

The PDS measurements of smoke showed a good comparison to the soiled tape results for levels from 2-10 mg/m³. Below 1 mg/m³, the soiled tape meter is very inaccurate and the comparison was poor. The TEOM and PDS instruments showed similar results measuring

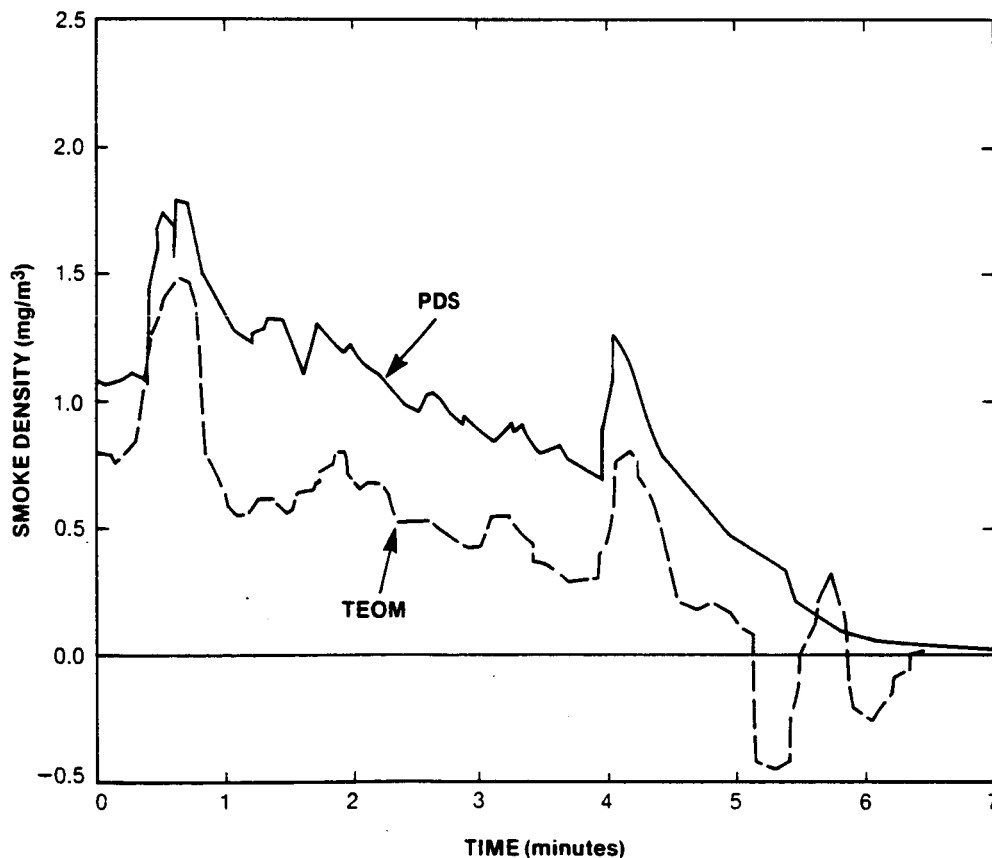


Figure 2-20. Comparison of the time history of smoke density from the PDS and TEOM instruments

the time history of the smoke generator output from 0.3 to 2 mg/m³. Below 0.3 mg/m³, the TEOM instrument would often oscillate, giving negative weights. The PDS instrument followed smoke signals down to levels as low as 50 μg/m³. The results of the NO₂ and smoke measurements demonstrate that the PDS meter can cover the smoke range of interest from 0.1 to 12 mg/m³ with good accuracy and linearity.

The desired frequency response of 1 sample per second given in Appendix A has been accomplished with the PDS system. All the smoke measurements were taken at a flow rate of 3 liters per minute, which is a residence time of 0.8 seconds in the PDS cell (39 cc volume). The smoke measurements were taken with a lock-in amplifier time constant of 30 seconds because of the erratic fluctuations in the smoke generator output. However, the NO₂ measurements simulating smoke absorption were all taken with a time constant of 1 second (except for the very lowest level, 0.2 mg/m³ which was measured with a time constant of 3 seconds).

The major problem with the PDS instrument is interference from NO₂ (16 ppm of NO₂ is equivalent to 1 mg/m³ of smoke). This interference could be alleviated by using a different laser wavelength for the pump beam. A Nd:Yag laser (1.06 μm wavelength) is a possible choice since the NO₂ absorption is negligible at this wavelength. In addition, a Nd:Yag laser with 4 W continuous power at 1.06 μm is inexpensive. The only interfering gas at 1.06 μm is water vapor. The absorption coefficients of Nd:Yag light at 1.06 μm were measured to be 12% per cm in liquid water at room temperature. Assuming the molecular absorption for water vapor is the same, the specific absorption coefficient of water is:

$$A_{\text{H}_2\text{O}} = \frac{0.12 \text{ cm}^{-1}}{1 \text{ g/cm}^3} = 1.2 \times 10^{-5} \frac{\text{m}^2}{\text{g}} \quad (2-28)$$

This is almost 10⁶ times lower than the absorption coefficient of smoke at the same wavelength (≈ 10 m²/g). Water absorption equivalent to 100 μg/m³ of smoke is:

$$\rho_{\text{H}_2\text{O}} = 100 \mu\text{g/m}^3 \frac{10 \text{ m}^2/\text{g}}{1.2 \times 10^{-5} \text{ m}^2/\text{g}} = 83 \text{ g/m}^3 \quad (2-29)$$

However, the amount of water vapor in an engine exhaust is not small. Table 2-3 shows some typical values of water absorption. The conditions set in Appendix A are shown (350 kPa, 430 K, 16% water) and the light absorption is substantial when measuring small levels of smoke (water absorption equivalent to 0.34 mg/m³ of smoke). However, a PDS meter using an ice trap (commonly used in gas sampling system) would reduce the water absorption to negligible values (5.4 μg/m³ of equivalent smoke) as seen in Table 2-3. These absorption values are preliminary since liquid water values have been used and there is no correction for pressure broadening of the molecular lines.

The PDS cell did require cleaning of the windows to improve the light transmission of the cell. Since the average laser power in the cell was measured to correct the PDS signal, the contamination reduced only the signal-to-noise ratio. Designs with window purging would be easy to construct to prevent any reduction in signal-to-noise ratio due to window contamination.

Table 2-3
Water Absorption at 1.06 μm

P (kPa)	T (K)	Relative Humidity (%)	$X_{\text{H}_2\text{O}}$ (%)	$\rho_{\text{H}_2\text{O}}$ (g/m ³)	Water Absorption (m ⁻¹)	Equivalent Smoke ($\mu\text{g}/\text{m}^3$)
101	273	100	0.6	4.5	5.4×10^{-5}	5.4
101	294	50	1.2	9.3	1.1×10^{-4}	11.0
350*	430*	-	16*	282	3.4×10^{-3}	340

*Conditions set in "General Smoke Meter Requirements" (Appendix A).

Section 3

SUMMARY AND CONCLUSIONS

Two new optical smoke meters, modulated transmission (MODTRAN) and photothermal deflection spectroscopy (PDS), have been tested experimentally. Both techniques have the advantage of measuring optical absorption of smoke, which is closely related to the smoke density. The MODTRAN technique is a variation on a direct transmission measurement where smoke is passed through a transmission cell and the smoke density is modulated by a speaker. The fluctuating component of the optical transmission, which is directly proportional to the light extinction and the smoke density, is measured. The PDS technique is based on heating a probe laser beam with modulated pump laser light which is absorbed by the smoke. The smoke-laden gas is alternately heated and cooled by the action of the modulated pump laser beam, which deflects the probe laser beam. The probe beam deflection is proportional to the optical absorption and the smoke density. The performance of these two techniques is evaluated against a set of ideal smoke meter criteria called the "General Smoke Meter Requirements" given in Appendix A. The results of this evaluation are discussed in the following section and summarized in Table 3-1.

1. **Accuracy.** Within the instrument range of each technique, the accuracy of both instruments is estimated to be about $\pm 10\%$. Most of this uncertainty is in the specific absorption of smoke, which is found to vary for different types of smoke.¹²
2. **Range.** The MODTRAN instrument was unable to resolve the low smoke levels (0.1 to 3 mg/m³), and improvements in the technique are not expected to increase the sensitivity to the desired lower limit of 0.1 mg/m³. The PDS meter covered the entire range, measuring smoke down to 0.05 mg/m³ and well above 12 mg/m³ with good linearity and signal-to-noise ratio.
3. **Particle Size.** Both techniques measure optical absorption of smoke, which is independent of the particle size distribution for small particles (below 0.1 μm diameter) that absorb light in the Rayleigh regime. Smoke samples that consist of primarily large particles (0.5 to 1.0 μm) may result in inaccurate measurements of the smoke density. Most of the measurements of particle size in jet engines indicate smoke particle sizes in the Rayleigh regime. Large particles are found only in the older engines with high smoke levels.
4. **Frequency Response.** The optical signal from both techniques has a fast time response, and 1 Hz signal sampling times are easily achieved. For the MODTRAN instrument the sample flow system limits the times response because the sample cell is large (3.8 liters). At typical sample flow rates of 12 liters/min, the flow residence time is about 20 seconds. The PDS sample cell is much smaller (39 cc), and the typical flow residence time in the cell is less than 1 second.
5. **Digital Control.** Both the MODTRAN and PDS technique produce analog signals that can be easily digitized.
6. **Exhaust Sample Conditions** (350 kPa, 430 K, 16% H₂O) The MODTRAN system would require major design changes to operate at high temperature and high pressure. A more rugged acoustic driver and pressure sensor would be needed to replace the speaker and microphone. The PDS system has a passive cell that is easily adaptable to high-pressure and high-temperature operation.
7. **Stability.** Both techniques show good stability in maintaining calibration. There are some problems with calibration drift and window contamination, but these could be al-

leviated with straightforward design changes.

8. **Smoke Discrimination.** Since both techniques measure smoke absorption of visible light ($\approx 0.5 \mu\text{m}$), they have good specificity to smoke. The main interference is due to NO_2 (16 ppm of NO_2 is equivalent to 1 mg/m^3 of smoke). The PDS technique could use a Nd:Yag pump laser at $1.06 \mu\text{m}$ wavelength where the NO_2 absorption is negligible. Possible interference by water vapor absorption at $1.06 \mu\text{m}$ could be eliminated by condensing the water vapor out of the sample gas with a cold trap.
9. **Engine Environment.** (Test cell conditions of 255-325 K temperature, 160 dB acoustic noise, $50 \mu\text{m}$ (0-200 Hz) vibration) Both techniques have been chosen because of their ability to operate in a high level of acoustic noise. The phase-sensitive detection used in both methods gives good discrimination against background noise. However, successful operation of these optical systems with 160 dB of acoustic noise seems unlikely. A better estimate may be 120 dB. The vibration sensitivity of these systems needs to be tested. The most likely application of these smoke meters is in a quieter room adjacent to the test cell that has the harsh conditions described above.
10. **Calibration.** Both systems have good calibration methods using measured amounts of NO_2 to simulate smoke absorption.
11. **Reliability and Maintenance.** Both systems are more complex than the soiled tape meter. However, the optical configurations are relatively simple. An industrial instrument could be designed which featured simplicity of operation and reliability.

Clearly from these results, the PDS meter has been demonstrated to meet nearly all the requirements of an ideal smoke meter. The PDS meter shows outstanding sensitivity to smoke (down to 0.05 mg/m^3), good linearity, and good frequency response. Use of a Nd:Yag laser at $1.06 \mu\text{m}$ should alleviate the optical interference of NO_2 which is often present in jet engine exhausts.

Although the MODTRAN system showed good linearity, it was unable to measure smoke levels below 3 mg/m^3 . Lower sensitivity is needed since modern jet engines are producing smoke levels below 1 mg/m^3 . Also the MODTRAN cell lacked good frequency response since the sample cell size was large.

Table 3-1
Smoke Meter Performance

Smoke Meter Requirement	MODTRAN	PDS
1. Accuracy ($\pm 10\%$)	Good ($\pm 10\%$)	Good ($\pm 10\%$)
2. Range (0.1-12 mg/m ³)	Poor (3 to > 12 mg/m ³)	Excellent (0.05 to > 12 mg/m ³)
3. Particle Size (0.03-1 μm)	Good	Good
4. Frequency Response (1 Hz)	Poor (Large cell size)	Good (1 Hz)
5. Digital Control	Good	Good
6. Exhaust Sample Conditions (350 kPa, 430 K, 16% H ₂ O)	Not established	Not established
7. Stability	Good	Good
8. Smoke Discrimination	NO ₂ Interference	NO ₂ Interference
9. Engine Environment (160 dB acoustic noise)	Unlikely (120 dB maximum)	Unlikely (120 dB maximum)
10. Calibration Method	Good	Good
11. Reliability and Maintenance	Good	Good

Appendix A

GENERAL SMOKE METER REQUIREMENTS

1. System inaccuracy must be less than 10% of reading or 0.2 milligrams/cubic meter, whichever is higher, with resolution of 5% of reading. System inaccuracy is defined as the difference, expressed as a percent of the known concentration, between a known mass concentration input and the smoke meter output reading.
2. The system must be capable of meeting the accuracy requirements over a mass concentration range from 0.1 milligram/cubic meter to 12 milligrams/cubic meter.
3. The system must be capable of meeting the accuracy requirements over a particle size range of from 0.03 micrometers to 1.0 micrometers.
4. The system must be capable of at least 1 mass concentration reading per second assuming a properly conditioned sample delivered to the instrument input.
5. The system design must allow for digital control of all functions and for digital readout of the system output.
6. The system must be capable of measuring the carbon content of a sample that is 16% water vapor by volume that has a pressure of 350 kPa and a gas temperature of 430 K.
7. The system must have sufficient stability so that accuracy can be maintained with system re-standardization on a one-half hour cycle. System must have a convenient and reliable standardization system.
8. It is highly desirable that the system be able to differentiate between carbon particles that are smoke and other constituents including gases and non-smoke particles introduced into but not consumed by the combustion process.
9. The system must be packaged so that it can safely operate within specifications while located close to the test vehicle/jet engine in order to maintain short sampling lines. The control may be located in a less severe environment. The expected test cell environmental conditions include:

Temperature	255-325 K
Acoustic Noise	160 dB
Vibration	50 micrometers (0-200 Hz)

10. The system should have a reliable calibration method.
11. The system must be reliable and simple to operate, and must require a minimum training time for operating technicians.

REFERENCES

1. "Exhaust Emissions from Gas Turbine Aircraft Engines," Sub-Council Report, National Industrial Pollution Control Council, February, 1971.
2. Bahr, D.W., "Control and Reduction of Aircraft Turbine Engine Exhaust Emissions," *Emissions from Continuous Combustion Systems*, W. Cornelius and W.G. Agnew, editors, Plenum Press, New York, 1972.
3. Naegeli, D.W., and C.A. Moses, "Fuel Microemulsions for Jet Engine Smoke Reduction," *J. Eng. Power.*, Trans. ASME, *105*, pp. 18-23, 1983.
4. Shaffernocker, W.M., and C.M. Stanforth, "Smoke Measurement Techniques," Air Transportation Meeting, SAE Paper No. 680346, New York, May, 1968.
5. Aerospace Recommended Practice, ARP 1179A, "Aircraft Gas Turbine Engine Exhaust Smoke Measurement," Society of Automotive Engineers, revised June, 1980.
6. Faxvog, F.R. and D.M. Roessler, "Optoacoustic Measurements of Diesel Particulate Emissions," *J. Appl. Physics*, *50*, pp. 7880-7882, 1979.
7. Japar, S.M. and A.C. Szkarlat, "Measurement of Diesel Vehicle Exhaust Particulate Using Photoacoustic Spectroscopy," *Comb. Sci. Tech.*, *24*, pp. 215-219, 1981.
8. Pitz, R.W., Penney, C.M., Stanforth, C.M., and Shaffernocker, W.M., "Advanced Smoke Meter Development: Survey and Analysis" NASA Report No. CR-168287, November, 1984.
9. Champagne, D.L. "Standard Measurement of Aircraft Gas Turbine Engine Exhaust Smoke," ASME Paper No. 71-GT-88, Gas Turbine Conference, Houston, Texas, March, 1971.
10. Melling, A. and J. H. Whitelaw, "Optical and Flow Aspects of Particles," *The Accuracy of Flow Measurements by Laser Doppler Methods*, Proceedings of the LDA-Symposium, P. Buchhave et al, editors, Copenhagen, 1975.
11. Mazumder, M. K. and K. J. Kirsch, "Flow Tracing Fidelity of Scattering Aerosol in Laser Doppler Velocimetry," *Appl. Optics*, *14*, p. 894-901, 1975.
12. Roessler, D.M. and F.R. Faxvog, "Optical Properties of Agglomerated Acetylene Smoke Particles at 0.5145- μm and 10.6- μm Wavelength," *J. Opt. Soc. Am.*, *70*, pp. 230-235, 1980.
13. Wang, J.C.F., H. Patashnick and G. Rupprecht, "A New Real-Time Isokinetic Dust Mass Monitoring System," *J. Air Poll. Contr. Assoc.*, *30*, pp. 1018-1021, 1980.
14. Rutter, S., "A Comparison of Techniques for Measuring Particulate Emissions of a Gas Turbine Engine," ASME Joint Power Generation Conference, ASME Paper No. 83-JPGC-GT-14, Indianapolis, IN, September 25-29, 1983.
15. Lee, T.G.K., and G.W. Mulholland, "Carbonaceous Aerosol Generator for Inhalation Studies," EPA Report No. EPA-600/1-80-014, February, 1980.
16. Fournier, D., A. C. Boccaro, N. M. Amer, and R. Gerlach, "Sensitive In Situ Trace-gas Detection by Photothermal Deflection Spectroscopy," *Appl. Phys. Lett.*, *37*, pp. 519-521, 1980.
17. Sell, J. A., "Quantitative Photothermal Deflection Spectroscopy in a Flowing Stream of Gas," *Appl. Opt.*, *23*, 1586-1597 (1984).

18. Sell, J. A., "Photoacoustic and Photothermal Deflection Spectroscopy of Propane at CO₂ Wavelengths," *Appl. Opt.*, *24*, pp. 152-153, 1985.
19. Rose, A., J. D. Pyrum, C. Muzny, G. J. Salamo and R. Gupta, "Application of the Photothermal Deflection Technique to Combustion Diagnostics," *Appl. Opt.*, *21*, pp. 2663-2665, 1982.
20. Kizirnis, S. W., R. J. Brecha, B. N. Ganguly, L. P. Goss, and R. Gupta, "Hydroxyl (OH) Distributions and Temperature Profiles in a Premixed Propane Flame Obtained by Laser Deflection Techniques," *Appl. Opt.*, *23*, pp. 3873-3881, 1984.
21. Boccara, A. C., D. Fournier, W. Jackson, and N. M. Amer, "Sensitive Photothermal Deflection Technique for Measuring Absorption in Optically Thin Media," *Opt. Lett.*, *5*, pp. 377-379, 1980.
22. Boccara, A. C., D. Fournier, and J. Badoz, "Thermo-optical Spectroscopy: Detection by the 'Mirage Effect'," *Appl. Phys. Lett.*, *36*, pp. 130-132, 1980.
23. Jackson, W. B., N. M. Amer, A. C. Boccara, and D. Fournier, "Photothermal Deflection Spectroscopy and Detection," *Appl. Opt.*, *20*, pp. 1333-1344, 1981.
24. Weinberg, F. J., *Optics of Flames*, Butterworth, Washington, DC, p. 24, 1963.
25. Silicon Detector Corporation, 855 Lawrence Dr., Newbury Park, CA 91320.
26. Hall, T. C., Jr., and F. E. Blacet, "Separation of the Absorption Spectra of NO₂ and N₂O₄ in the Range of 2400-5000 Å," *J. Chem. Phys.*, *20*, pp. 1745-1749, 1952.

CONTRACT REPORT DISTRIBUTION LIST

Instrumentation and Control Technology Office

NASA Lewis Research Center
Attn: R. C. Anderson
Mail Stop 77-1
Cleveland, OH 44135
(25 copies)

Air Force Wright Aeronautical
Laboratory
Attn: R. Cox/POTC
Wright Patterson AFB, OH 45433

NASA Lewis Research Center
Attn: Dr. A. Spence
21000 Brookpark Road
Cleveland, OH 44135
Mail Stop 500/305

Air Force Wright Aeronautical
Laboratory
Attn: William Stange/POTC
Wright Patterson AFB, OH 45433

NASA Lewis Research Center
Attn: Gerald A. Boulanger
21000 Brookpark Road
Cleveland, OH 44135
Mail Stop 500/305

Air Force Wright Aeronautical Laboratory
Attn: M. Roquemore/POSF
Wright Patterson AFB, OH 45433

NASA Scientific and Technical
Information Facility
Attn: Acquisitions Branch
P.O. Box 8757
B.W.I. Airport, Md 21240
(22 copies)

Naval Air Propulsion Test Center
Attn: Guy Mangano/Code PE42
Trenton, NJ 08628

NASA Lewis Research Center
Attn: Library, M.S. 60/3
21000 Brookpark Road
Cleveland, OH 44135
(2 copies)

Naval Air Propulsion Test Center
Attn: James Zidzik
Trenton, NJ 08628

NASA Lewis Research Center
Attn: Report Control Office,
Mail Stop 60/1
21000 Brookpark Road
Cleveland, OH 44315

UTRC/OATL
Attn: John T. Carroll
Bldg. 30, MS R-23
Palm Beach Gardens Facility
West Palm Beach, FL 33402

General Electric Company
Aircraft Engine Group
Evendale, OH 45215
Attn: Wayne Shaffernocker, MSH-78
Ronald Weise, MSH-78
William Stowell

Lewis Engineering Company
Attn: C.B. Stegner
238 Wate Street
Naugatuck, CT 06770

Stanford University
Attn: Dr. R.J. Moffatt
Asst. Prof., Mech. Engr.
Dir. Thermoscience Measurement Center
Stanford, CA 94305

Arnold Engineering Development Center
Attn: Marshall Kingery
Arnold Air Force Station, TN 37389

Hitec Corporation
Attn: Steve Wnuk
Nardone Industrial Park
Westford, MA 01886

General Electric Company
Attn: George Leperch, A129dD
Aircraft Engine Group
1000 Western Avenue
Lynn, MA 01910

General Electric Company
Attn: Ronald J. Casagrande
Aircraft Equipment Division
50 Fordham Road
Wilmington, MA 01887

Allison Gas Turbine Operations
Attn: John Custer, W-16
General Motors Corporation
P.O. Box 894
Indianapolis, IN 46206

Allison Gas Turbine Operations
Attn: Ken Cross
P.O. Box 894
Indianapolis, IN 46206

Allison Gas Turbine Operations
Attn: David Willis
General Motors Corporation
P.O. Box 894
Indianapolis, IN 46206

Allison Gas Turbine Operations
Attn: Ralph Fox
General Motors Corporation
P.O. Box 894
Indianapolis, IN 46206

Battelle Columbus Laboratories
Attn: Ross G. Luce
Energy & Thermal Tech. Section
Columbus, OH 43201

Teledyne CAE
1350 Laskey Road
Toledo, OH 43612
Attn: R. Hugh Gaylord
Joseph Pacholec

FluiDyne Engr. Corporation
Attn: T. Matsuura
5900 Olson Memorial Highway
Minneapolis, MN 55422

AVCO Corporation
Attn: E. Twarog, Manager
Electronics and Instr.
Lycoming Division
550 South Main Street
Stratford, CT 06497

Thermonetics Corporation
Attn: H.J. Poppendiek
1028 Garnet Avenue
San Diego, CA 92109

Battelle Columbus Laboratories
Attn: M.M. Lemcoe
505 King Avenue
Columbus, OH 43201

Peter K. Stein
4602 East Monterosa
Phoenix, AZ 85018

Pratt & Whitney Aircraft
Main Plant
P.O. Box 2691
West Palm Beach, FL 33402
Attn: John Prosser (MS C-04)
William Watkins

National Bureau of Standards
Attn: Ken Kreiger
Washington, DC 20234

National Bureau of Standards
Attn: George Burns
Inst. for Basic Research
Washington, DC 20234

General Electric Company
Attn: Dr. David Skelley
Bldg. K-1, Room KWC1532
P.O. Box 8
Schenectady, NY 12301

Garrett Turbine Engine Company
Attn: N. Fred Pratt
P.O. Box 5217
Phoenix, AZ 85010

Boeing Aerospace Company
Attn: Darrell R. Harting
Engineering Laboratories
Seattle, WA 98124

Engelhard
Attn: Ronald G. Braun
Engelhard Industries Div.
228 East 10th Street
Newport, KY 41075

Williams International
2280 West Maple Road
Walled Lake, MI 48088
Attn: Henry Moore, Head,
Instr. Dept.
J.H. Johnston

Virginia Polytechnic Institute
and State University
Attn: W.F. O'Brien, Jr.
Mechanical Engineering Dept.
Blacksburg, VA 24061

Naval Post Graduate School
Attn: Prof. R.P. Shreve
Department of Aeronautics (Code 67)
Monterey, CA 93940

Pennsylvania State University
Attn: Prof. B. Lakshminarayana
233 Hammond Building
University Park, PA 16802

Kulite Semiconductor Products, Inc.
Attn: John R. Hayer
1039 Hoyt Avenue
Ridgefield, NJ 07657

Bolt Beranek and Newman, Inc.
Attn: Richard E. Hayden
50 Moulton Street
Cambridge, MA 02138

Air Force Wright Aeronautical
Laboratory
Attn: Mr. Charles Bentz/POTC
Hot Section Technology
Wright Patterson AFB, OH 45433

AVCO Corporation
Attn: Mr. K. Collinge, Dir. of Research
IRAD Mechanical Projects Manager
Lycoming Division
550 South Main Street
Stratford, CT 06497

Eaton Corporation
Attn: Mr. Lamont Eltinge
P.O. Box 766
Southfield, MI 48037

Public Service Elect. & Gas Company
Attn: Dr. Melvin L. Zwillenberg
Research & Development Dept.
80 Park Plaza
Newark, NJ 07101

Raychem Corporation
Attn: Dr. David C. Chappellear
Director of Corporate Res. & Dev.
300 Constitution Drive
Menlo Park, CA 94025

Fabrication Development Laboratory
Attn: Mr. Hugh W. Bradley, Jr.
Owens/Corning Fiberglas
Technical Center
Granville, OH 43023

Xerox Electro-Optical Systems
Attn: Mr. Clifford I. Cummings
Manager, Intelligence & Reconnaissance
1616 North Fort Myer Drive, 16th Floor
Arlington, VA 22209

Construction Materials Support Group
Attn: Mr. J.W. Scott
Owens/Corning Fiberglas
CMG Process Technology Laboratory
Granville, OH 43023

Babcock & Wilcox R&D Division
Attn: Harold Wahle
P.O. Box 835
Alliance, OH 44601

Caterpillar Tractor Company
Attn: Mr. Donald Wilson
Technical Center, Building F
100 Northeast Adams Street
Peoria, IL 61629

NASA Headquarters
Attn: M/Paul N. Herr
Washington, DC 20546

Massachusetts Inst. of Technology
Attn: Dr. Alan Epstein, Rm 31-266
Cambridge, MA 02139

Sverdrup (AEDC)
Attn: Paul McCarty
Arnold AFB, TN 37389

Rosemont, Inc
Attn: Mr. Larry N. Wolfe
Mail Stop F-15
P.O. Box 959
Burnsville, MN 55337

Thermogage, Inc.
Attn: Charles E. Brookley
330 Allegany Street
Frostburg, MD 21534

Hycal Engineering
Attn: William Clayton
12105 Los Nietos Road
Sante Fe Springs, CA 90670

Medtherm Corporation
Attn: Larry Jones
P.O. Box 412
Huntsville, AL 35804

Rocketdyne
Attn: Dr. John C. Lee
6633 Canoga Avenue
Canoga Park, CA 91304

Combustion Engineering
Attn: John Fishburn
Dept. 9005-03D1
Windsor, CT 06095

RdF Corporation
Attn: Frank Hines
23 Elm Avenue
Hudson, NH 03051

RdF Corporation
Attn: Frank Hines
23 Elm Avenue
Hudson, NH 03051

NASA Langley Research Center
Attn: R.E. Wright, Jr. (MS-234)
Hampton, VA 23665

NASA Langley Research Center
Attn: S.L. Ocheltree (MS-235A)
Hampton, VA 23665

Babcock & Wilcox R&D Division
Attn: John Berthold
P.O. Box 835
Alliance, OH 44601

Applied Sensors International
Attn: Richard Stillmaker
7834 Palace Drive
Cincinnati, OH 45242

Carnegie-Mellon University
Attn: Dr. Norman Chigier
Dept. of Mechanical Engineering
Pittsburgh, PA 15213

Calspan Field Services, Inc./AEDC Div.
Attn: C.T. Kidd
Arnold Air Force Station, TN 37389

Physical Sciences Dept.
Attn: M.G. Dunn
Arvin/Calspan Adv. Tech. Ctr.
Buffalo, NY 14225

Eaton Corporation
Attn: Howard K. Cooper
Electronic Instrumentation Division
(Ailtech Strain Sensors)
5340 Alla Road
Los Angeles, CA 90066

Naval Air Propulsion Test Center
Attn: Guy Mangano/Code PE42
Trenton, NJ 08628

Naval Air Propulsion Test Center
Attn: James Zidzik
Trenton, NJ 08628

1. Report No. CR--179459		2. Government Accession No.		3. Recipient's Catalog No.	
4. Title and Subtitle Advanced Optical Smoke Meters for Jet Engine Exhaust Measurement				5. Report Date September 1986	
				6. Performing Organization Code	
7. Author(s) Robert W. Pitz				8. Performing Organization Report No.	
				10. Work Unit No.	
9. Performing Organization Name and Address General Electric Company Corporate Research and Development P. O. Box 8 Schenectady, New York 12301				11. Contract or Grant No. NAS3-24084	
				13. Type of Report and Period Covered Final Report	
12. Sponsoring Agency Name and Address National Aeronautics and Space Administration 21000 Brookpark Road Cleveland, OH 44135				14. Sponsoring Agency Code 505-62-01	
15. Supplementary Notes Project Manager, Robert C. Anderson Instrumentation & Control Technology Office NASA Lewis Research Center, Cleveland, Ohio 44135					
16. Abstract <p>Smoke meters with increased sensitivity, improved accuracy, and rapid response are needed to measure the smoke levels emitted by modern jet engines. The standard soiled tape meter in current use is based on filtering, which yields long term averages and is insensitive to low smoke levels. Two new optical smoke meter techniques that promise to overcome these difficulties have been experimentally evaluated: modulated transmission (MODTRAN) and photothermal deflection spectroscopy (PDS). Both techniques are based on light absorption by smoke, which is closely related to smoke density. They are variations on direct transmission measurements which produce a modulated signal that can be easily measured with phase sensitive detection. The MODTRAN and PDS techniques were tested on low levels of smoke and diluted samples of NO₂ in nitrogen, simulating light absorption due to smoke. The results are evaluated against a set of ideal smoke meter criteria that include a desired smoke measurement range of 0.1 to 12 mg/m³ (smoke numbers of 1 to 50) and a frequency response of 1 per second. The MODTRAN instrument is found to be inaccurate for smoke levels below 3 mg/m³ and is able to make a measurement only about once every 20 seconds because of its large sample cell. The PDS instrument meets nearly all the characteristics of an ideal smoke meter: it has excellent sensitivity over a range of smoke levels from 0.1 to 20 mg/m³ (smoke numbers of 1 to 60) and good frequency response (1 per second).</p>					
17. Key Words (Suggested by Author(s)) Jet Exhaust/Smoke/Optical Measurement/ Laser Applications/Measuring Instruments			18. Distribution Statement Unclassified-unlimited		
19. Security Classif. (of this report) Unclassified		20. Security Classif. (of this page) Unclassified		21. No. of pages	22. Price*